QUATERNARY SEISMIC STRATIGRAPHY OF THE HAMILTON SPUR: A SEDIMENT DRIFT ON THE LABRADOR CONTINENTAL SLOPE

Shawn Goss

Submitted in Partial Fulfillment of the Requirements
for the Degree of Bachelor of Science, Honours

Department of Earth Sciences
Dalhousie University
Halifax, Nova Scotia
March 2006

Abstract

The Hamilton Spur is a large late Cenozoic sediment drift feature, that trends northeastward between 300 m and 3000 m water depth on the Labrador continental margin. The objective of this study is to understand the Quaternary development of this large deep water drift which formed by the southward flowing Labrador Current and Western Boundary Undercurrent reworking and depositing continental margin sediments. To gain a better understanding of the processes that directly influence the Hamilton Spur, 289 km of single channel air gun seismic reflection, Huntec subbottom data and three piston cores were examined. The study mapped a major near surface unconformity that marks the initiation of the Labrador Current, defined by the erosion of a pre-existing sediment drift. Overlying the unconformity, 5 key horizons were mapped indicating a southward migration of the Hamilton Spur. The northern flanks of the spur are subjected to intense current velocities and current reworking, with subsequent deposition on the southern flanks of the ridge where decreases in current velocities cause a loss of sediment suspension within the water column, evident in thickened units. Six seismic facies have been established on the Hamilton Spur indicating variations in depositional environments over the spur depending on depth and location to current axis. Piston cores support the idea of current influenced deposition in which increased sediment thickness is observed. Cores contain 5 lithofacies, indicating changes in depositional patterns over the ridge. The outer margin and the upper slope (~300-1200 m) of the northern flanks are controlled mainly by the deeper Labrador Current component where clays and silty sediments are subjected to winnowing, leaving more coarse sands and lag deposits. The middle slope region (~1200 m) is considered to be unaltered by currents defined by a "zone of minimum motion". The lower base and northern flanks (1200-3000 m) are subject to the intense axis of the Western Boundary Under Current, responsible for considerable reworking of bottom material and the presence of considerable amounts of sands, and minor traces of silts. Seismic reflection data and piston cores collected support the idea of current influenced deposition, through bottom-sediment reworking by the intense southward flow of the Labrador Current and Western Boundary Undercurrent. Sedimentation processes such as mass transport deposits and glacial melt-water deposits followed the development of the unconformity. Under modern conditions, current intensity and sedimentation rates have decreased on the Spur, however the Hamilton Spur's depocenter continues its southward migration.

Key words: Labrador Current, Western Boundary Under Current, Seismic Reflection, Horizon, Piston Core

Table of Contents

Table of Figures

Table of Tables

Acknowledgements

I would like to thank first and foremost Dr. David Mosher for allowing me to participate on Hudson cruise 2005033B and his ability to keep his composure with me through this 8 month thesis ordeal. He provided me with valuable knowledge and skills I will carry with me the rest of my life. I have to thank Dr. Grant Wach for all his support and guidance throughout my last days here at Dalhousie. A much needed acknowledgement to Dr. David Piper, a truly gifted researcher in deepwater sediments. I'd like to thank those who I have annoyed with the famous statement "I got a quick question?" which turned into 30 minute conversations: Calvin Campbell, Gary Sonnichsen, Laurie Tremblay and Dave Scott among others. I would also like to thank Reed Schneider and Matt Robichaud who showed me the way into Geology. I cant forget to thank all my friends at Dalhousie and my two roommates Graham Reid, and John Sutherland who handled my stress the best they could over the past year. My Girlfriend Meghan Taylor also deserves to be acknowledged, she has given me wonderful inspiration and drive to accomplish some of the most daunting tasks that I have undertaken and continues to support me in every aspect of my studies. Last I have to acknowledge my parents for making this all possible, I couldn't have made it this far without them.

Chapter 1

Introduction

1.0 Introduction

Greater knowledge of deep water geological process is necessary for understanding sediment distribution patterns, paleoceanographic changes, and potential geohazards and constraints to offshore development. As research in deep water regions continues, it is increasingly observed that these are active sedimentological environments.

1.1 Scope & Objectives of the Project

The objective of this study is to understand the Quaternary development of a large deep water sediment drift deposit known as the Hamilton Spur; a major bathymetric feature of the Labrador continental margin formed by the Labrador Current and Western Boundary Undercurrent reworking and depositing continental margin sediments. Sedimentation patterns within the spur reflect changes in currents through time and across the feature.

1.2 Physiography

The Labrador margin consists of an outer shelf of banks and saddles separated from an irregular inner shelf by a deep marginal trough that marks the formational boundary between Precambrian rocks of Labrador and the Cretaceous- Cenozoic continental margin sediment wedge (Josenhans H.W., 1990). The Labrador Shelf is 50 km wide with a pronounced continental rise (Myers and Piper, 1988). The banks are described as being relatively flat-topped, at depths between 200-300 mbsl (meters below

sea level), the saddles are found to be approximately 400-550 mbsl and tend to shoal seaward from the marginal trough (Josenhans, H.W., 1990).

1.3 Previous Work

Few studies of the Quaternary geology of the Labrador Slope have been conducted to date. The Geological Survey of Canada conducted a series of seismic surveys starting in the mid to late 60's which revealed that the Hamilton Spur is a major sedimentary wedge. Industrial interests in the offshore basins off Canada's east coast during the 1970's and 80's resulted in several geophysical and geological surveys being conducted. These surveys included the acquisition of 1000's of km of multi-channel reflection data in the areas surrounding the Hamilton Spur. Myers (1986) and Myers and Piper (1988) provide an overview of the Cenozoic architecture of the region and recognized associations between bottom circulation and glaciations with regards to Spur development.

1.3.1 Study Area

The study area lies 200 km off the Labrador coast in the southwestern region of the Labrador margin (Figures 1.0 and 1.1) The Hamilton Spur is located at approximately 55° N, 54° W, trending east-west, with the Cartwright Saddle to the north-west and Hawks Saddle to the south-east. The shallow unit of the Hamilton Spur occurs in water depths of approximately 200-300 m, with the base occurring at 3000 m, covering an area of approximately 50 km^2. The Hamilton Spur produces a promontory feature in the margins topography and extends approximately 175 km long into the basin and is 125 km wide at its broadest point. The continental slope to the north of the study area trends in a

northwest-southeast direction. The slope gradient over the Spur is uniform from 500 m depth to 2000 m depth, beyond which it becomes more gentle. The slope is cut transversely my numerous deep sea canyons and troughs. The Spur protrudes sharply at approximately 54.0° latitude east of the Hamilton Bank where the contours trend east-west. From 500 m depth to 1500 m depth, the contours are fairly uniform in space; from 1500 m to 2500 m the contours increase in spacing down the Labrador Rise. To the south of the Hamilton Spur the slope trends back to follow a northwest-southeast direction, but is much steeper than the northern slope. Like the northern slope, there is uniform gradient from 500 m depth to 1500 m depth, becoming gentler from 1500 m depth to 2500 m depth. Similar to the north, the slope is intersected by deep-sea troughs and canyons trending east-west.

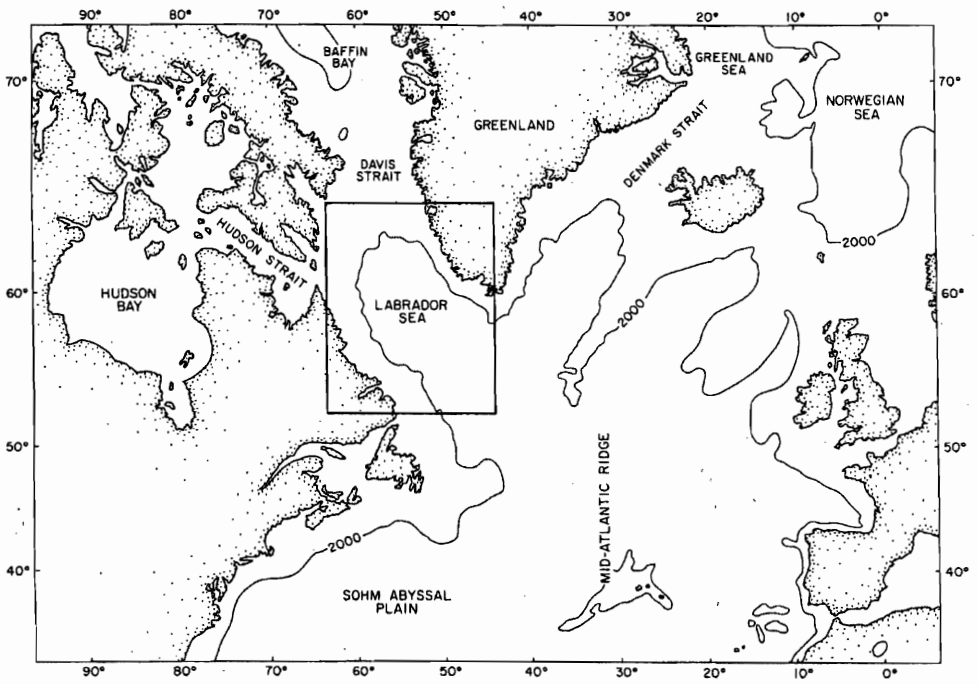

Figure 1.0 Map illustrating location of Labrador Sea (Modified after Myers and Piper, 1988).

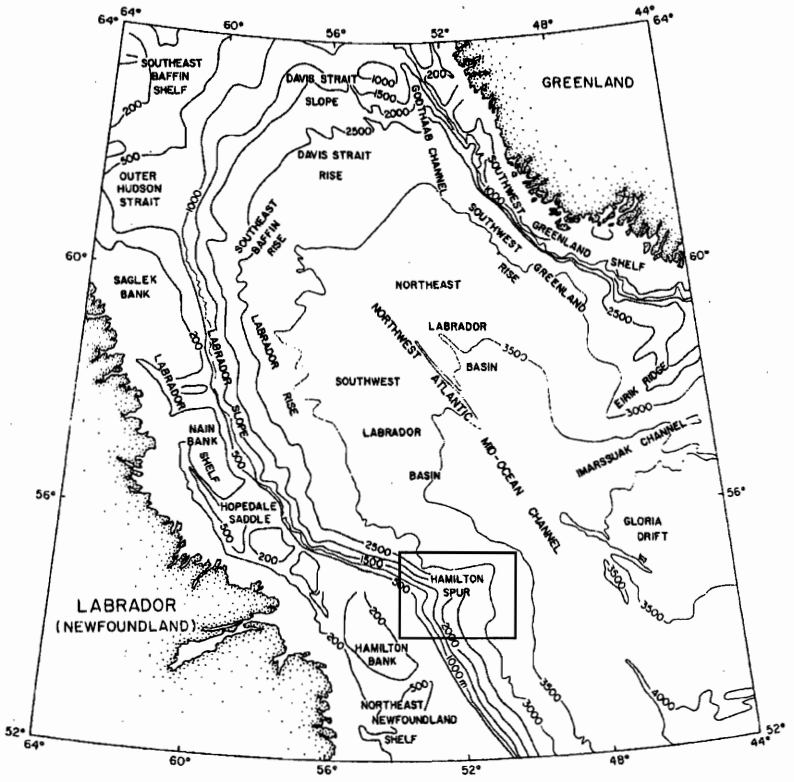

Figure 1.1 Map illustrating location of study area (modified after Myers and Piper, 1988)

1.4 - Geologic Setting:

The Labrador Sea is an arm of the North Atlantic Ocean that lies between Labrador and Greenland. The Labrador Sea was formed by rifting and sea-floor spreading in the late Cretaceous (Louden et al, 2004). Running parallel to the axis of the basin is the now extinct Mid-Labrador sea ridge. This ridge formed one limb of a triple junction that separated Greenland, North America, and Eurasia during the Late Cretaceous and early Tertiary. It stopped spreading between 45-39 mya, when the Mid-Atlantic ridge took its present form (Louden et al, 1996). The Labrador basin is an immense, oval tectonic depression in the southern part of the zone of extended cratonic and oceanic crust that connects the Atlantic to the Arctic basins. The basin has

topographically highly incised, glaciated crystalline rims of Precambrian rocks forming the coastal margins of Labrador. An uneven basin floor was formed due to the deep subsidence of a wide expanse of oceanic crust. A narrow zone of differentially extended, faulted, seaward inclined, cratonic basement separates the coastal basin rims from the oceanic basement floor (Balkwill et al, 1990). Sediment thickness in the central basin exceeds 2000 m, of which 1/3 was deposited in the last 3-4 Ma by mass flow processes (mainly turbidity currents) channeled through the North Atlantic Mid-ocean Channel (NAMOC) (Chough and Hesse, 1976). Sediments within the Labrador basin consist of mainly Cretaceous, Tertiary and Quaternary terrigenous clastic sediments. Large amounts of sediments were contributed from local upland erosion in the Late Phanerozoic during separation of the North American and Greenland plates, subjected to subsidence the oceanic realm was created (Balkwill et al, 1990). These sediments were derived from widespread erosion of central Canada during Pleistocene glaciations.

1.4.1 Tectonic and Stratigraphic Evolution

The Labrador Shelf has been characterized as an Atlantic type passive margin (Bally, 1981). The continental shelf is virtually flat as it protrudes towards the shelf break, where the continental slope steeply drops off. The inner parts of the shelf have been characterized as an erosional surface, developed on a Precambrian basement, whereas the outer shelf and slope have been determined to be a "thick prism of sea-ward dipping Cretaceous and younger terrigenous clastics " (Balkwill et al, 1990). The landward edge of the shelf lies on extended cratonic crust, which is known to contain large, elongate fault bounded wedges of Lower Cretaceous and lower Upper Cretaceous

syn-rift clastic sediments. The outer part of the shelf prism lies on Cretaceous and lower Tertiary basalts. It is not known whether these basalts are cratonic or oceanic.

The Labrador shelf has both sedimentary and volcanic rocks of Mesozoic-Cenozoic age. These rocks are split into three categories or megasequneces, resulting from three different tectonic regimes. These regimes include intra-cratonic rifting, cratonic separation of North America and Greenland, and ocean spreading. Another major factor in glacial evolution is the post-spreading massive subsidence of Labrador Sea oceanic crust.

1.4.2 Glacial History

The glacial history of the Labrador Shelf is complex. A lower till marks one or more major extensions of grounded ice that encompassed the entire Labrador shelf and is older then Late Wisconsinan (Josenhans and Piper, 1990). It has been interpreted that the sharp contact that exists between the upper and lower tills to be erosional due to glacial re-advance preceding deposition of the upper till, removing a large amount of the lower till from the inner shelf in water depths down to almost 800 m. The inner shelf and saddles at the time of deposition of the upper till acted as a restriction to the large ice mass and it does not appear to have extended seaward towards the banks. The upper till was deposited during ice retreat and it is somewhat over-consolidated and the upper surface is undulatory and ice scoured (Josenhans, and Piper, 1990). The ages of the two tills are uncertain. To date, the best possible hypothesis is that the upper till is of the Late Wisconsinan age corresponding to the Saglek glaciation, and the lower till is possible Middle Wisconsinan age.

Chapter 2

Methods

2.1 Introduction

Equipment used in this study included two seismic reflection systems and a piston coring system for sampling: 1) A single channel air gun seismic reflection profiling system, 2) a high resolution Huntec DTS sparker system, and 3) the AGC Giant Piston Corer. All equipment belonged to the Geological Survey of Canada (Atlantic) and has been used extensively in their deep water offshore investigations.

2.2 Seismic Reflection Surveying

Regional stratigraphic and sedimentologic analyses were conducted with data acquired from two different seismic profiling systems. Data from both systems were acquired simultaneously and survey track lines are shown in Figure 2.1. The majority of the project's seismic reflection data as well as AGC Long Cores were collected on CCGS Hudson Cruise 2005-O33B, July 22nd - August 20^{th,} 2005.

Seismic reflection systems are made up three of main components 1) a sound source, 2) a hydrophone receiver, 3) a recording apparatus. The source and the receiver are both deployed within the ocean and towed behind the vessel (Fig 2.2). The seismic source releases an acoustic signal, in the form of a pressure wave. The signal propagates through the water column and into the seafloor sediment. Upon impacting impedence changes (changes in velocity and density), some of the signal is reflected and the remainder is transmitted further into the underlying geology. The amount of energy that is reflected is directly related to the density and velocity contrasts. The portion of the

signal that propagates into the sediment follows a similar pattern, a portion reflecting off interfaces of impedance contrast and some transmitting further into the sediment until the signal is attenuated to the point where it is no longer detected. The reflected signals travel back through the water column where they are received by hydrophone receivers and are recorded by a shipboard digitizer.

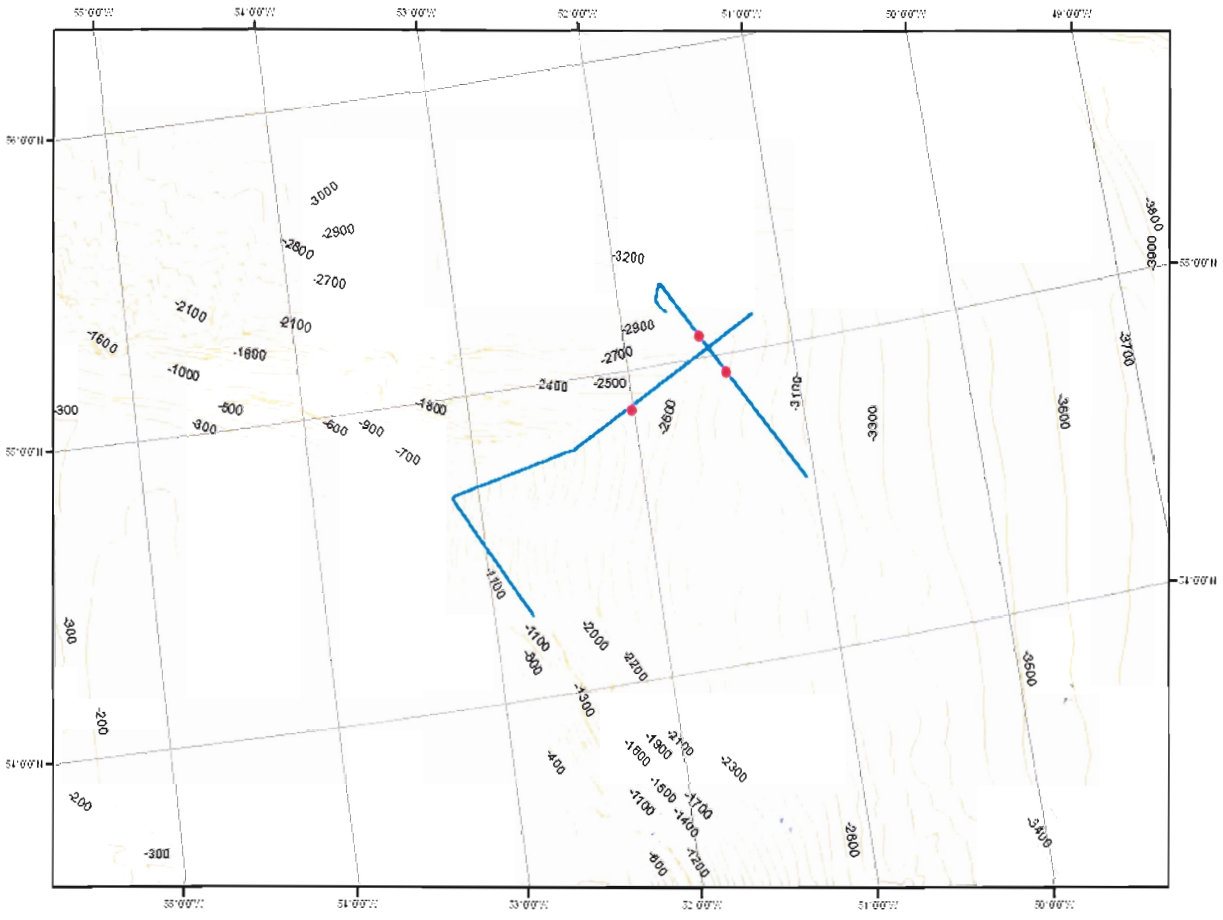

Figure 2.1 Single channel seismic lines acquired within the study area shown in blue, and piston core locations are indicated by red dots. Yellow lines represent contour depths within the study area. The seismic lines were acquired by the Geologic Survey Canada (Atlantic) on CCGS Hudson Cruise 2005033B

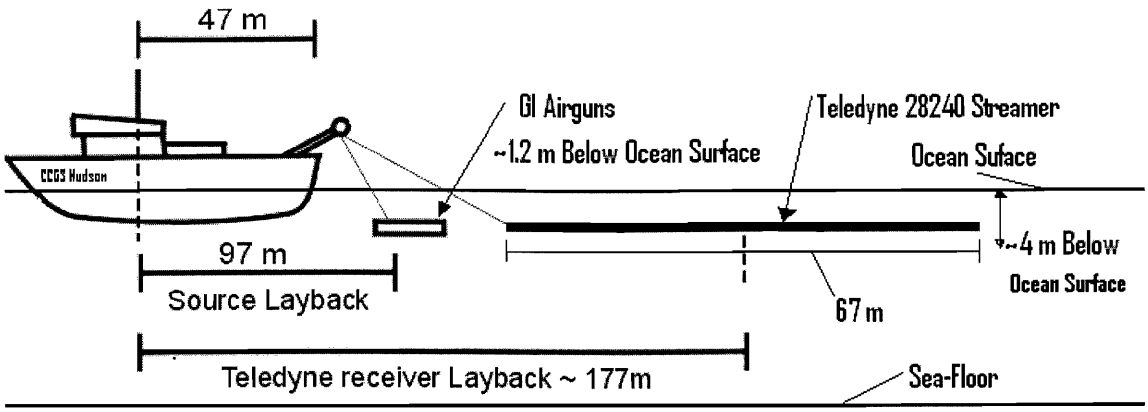

Figure 2.2 Diagram of the reflection seismic survey geometry (Modified after Mosher, 2005)

2.2.1 Single Channel Seismic Reflection Profiling

The single channel seismic reflection profiling system refers to the deeper penetrating system, used to investigate the overall structure and stratigraphy of the Hamilton Spur. The single channel seismic system used for this study consisted of a 2-gun array of 210 in^3 Sercel Generator Injector (GI) guns.

2.2.2 Seismic Source

The GI gun is a pneumatic device using a sudden release of compressed air to accelerate a water mass to generate a pressure wave. In the GI gun design, there are two chambers of compressed air. The "Generator" releases first, the resulting expanding air bubble generates the initial pressure wave. As the bubble expands over the "Injector" ports, the "Injector" chamber releases air to collapse the initial bubble. The injector therefore prevents secondary bubble oscillations that cause unwanted signals on the seismic profile (Mosher, 2005).

The two GI guns were hung from a 2.5 meter-long steel I-beam, mounted horizontally on chains approximately 2 meters apart, and 0.52 m below the I-beam. The sled is kept afloat by two large Norwegian floats, allowing the depth of the sled to be approximately 1.2 meters below the ocean surface (Fig 2.3)(Mosher et el , 2005). Each GI-gun is equipped with a blast phone, allowing for continuous monitoring of signals and delays between the generator and the injector pulses to obtain optimum bubble cancellation. Optimum frequencies were confined between 35-250 Hz.

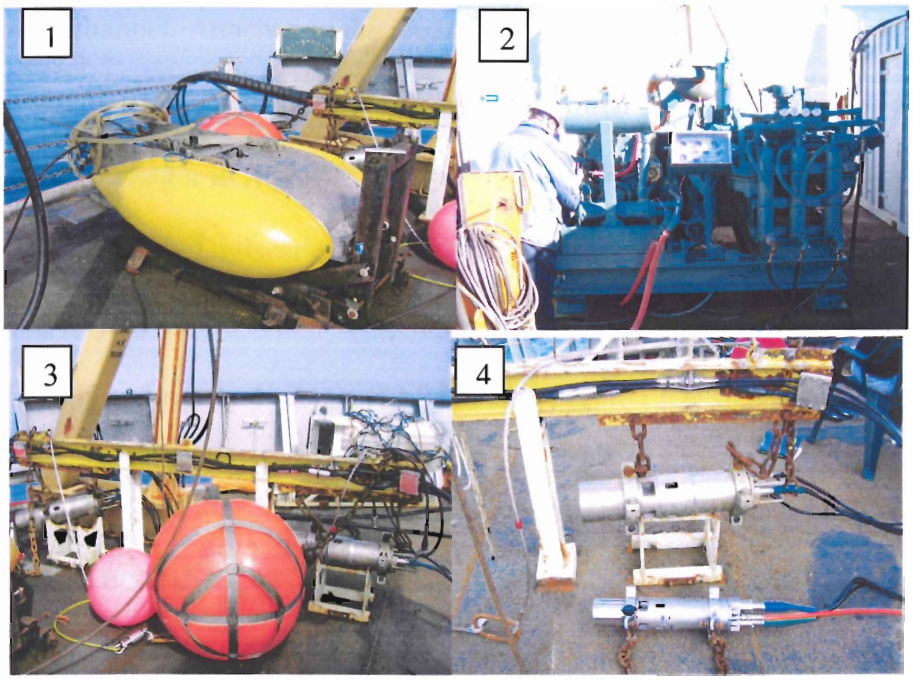

Figure 2.3 Some components of seismic acquisition system 1) Huntec Deep Tow System (DTS) 2) Price Model W2 Compressor 3) 2 x GI gun array configuration with Norwegian Floats 4) 2 different size GI guns.

2.2.3 Receivers

The Teledyne model 28420 streamer was used for receiving seismic signals. It measures 61 m (~200ft) in length. The first 8 m (~27 ft) of this 61 is a dead section, as well as the last 4.9 m (~16 ft) of the streamer tail. The remaining 42.4 m (~148.33ft) includes 2 interlaced sets of 3 groups of Teledyne B-1 acceleration canceling hydrophone cartridges. There are 16 individual hydrophones within a group, each separated by 1.0 m (3.14 ft). The companion interlaced group is exactly the same in dimensions, but with 0.23 m (.75 ft) of offset from the first group. The signals from each group are summed into one single channel. Attached to the lead of the Teledyne streamer is a DigiCourse DigiBird model 5010, applied each time before deployment. The "bird" acts as a self correcting depth manager in flight for the hydrophone streamer; controlled and monitored shipboard on a PC using Digiscan software. It is necessary to try and achieve tow depths similar to that of your sound source array to optimize signal bandwidth. It was maintained at approximately 4 meters (12 ft) depth. Figure (2.2) shows an illustration of the geometries of a seismic survey.

2.2.4 Digital Recording

Seismic signals from the hydrophones are not filtered or amplified when sent shipboard. The signals are received by the GSCDIGS digitizer and recorded on two channels: one raw and unfiltered, the other band pass filtered to eliminate unwanted noise. Seismic signals were digitally recorded with a sample interval of 250 μs (4000 Hz) for a time window ranging between 2-2.5 seconds. Before the seismic signals are written

to EPC hardcopy they pass through a Krohn-Hite Model 3750B 2-channel filter, band passed at 100 Hz and 500 Hz with 40db gain amplification. Navigation data were also read into the system and recorded with the seismic data. All seismic data were written to hard drive as industry standard SEG-Y format.

2.3 Huntec Deep Tow Systems (DTS)

The Huntec Deep Tow System (DTS) is a high resolution subbottom profiler, with an acoustic source, energy supply, motion sensor, streamer, and two receiving hydrophones located at the tow fish. There are two modes in which the acoustic source can be produced, boomer and sparker. Typically the boomer is the preferred mode, but for deep water or hard seafloor substratum a sparker attachment is used which increases the source energy. The sparker was used exclusively in this investigation. The fish is typically towed at a depth of 100 m, improvements in sparker source characteristics and repeatability are achieved by deep-towing the fish. The signals are received by a streamer attached to the rear of the fish and transmitted back to a shipboard processing unit. The streamer measures 7.32 m (12 ft), consisting of 24 hydrophone elements (AQ-16 cartridges). The signals are displayed in analogue hardcopy on an EPC9800 thermal chart recorder generally with a 500 ms sweep rate. The sparker data were filtered with a bandpass of 250 Hz to 2500 Hz. Digital recording of the raw Huntec data was performed by the GSCDIGS system, sampled at 50 μs (20 kHz) for a recording length of 500 ms. Typical firing rates were between 0.6-1.5 seconds depending on water depth.

2.4 Sediment Sampling

Three, 15m x 10 cm diameter piston cores were recovered in the study area with the AGC long Corer. The locations of these cores were based on Huntec profiles and bathymetry charts.

2.4.1 Piston Coring

The AGC Giant Piston Corer system was used to obtain 10 cm diameter sediment cores encased in a plastic liner (Fig 2.4, 2.5, 2.6). Barrel lengths are 3.05 meters (10 ft) and each core typically consists of 5 barrels. The core head is approximately 3 m in length and weights 1100 kg (2500 lbs). There is a split piston corer within the barrel which reduces the amount of resistance during penetration. The piston corer is controlled by a trip arm which releases when a trigger weight contacts the sea-floor (Fig 2.6). Upon release, the piston corer free falls through the water column for about 5 m. When it impacts the sea-floor, the barrel slides down around a piston. The piston, inside the core barrel, serves to create neutral pressure inside the corer, reducing sediment disturbance and assisting in greater corer penetration.

Figure 2.4 Piston Core deployment. (Photo from Hudson Cruise 2004)

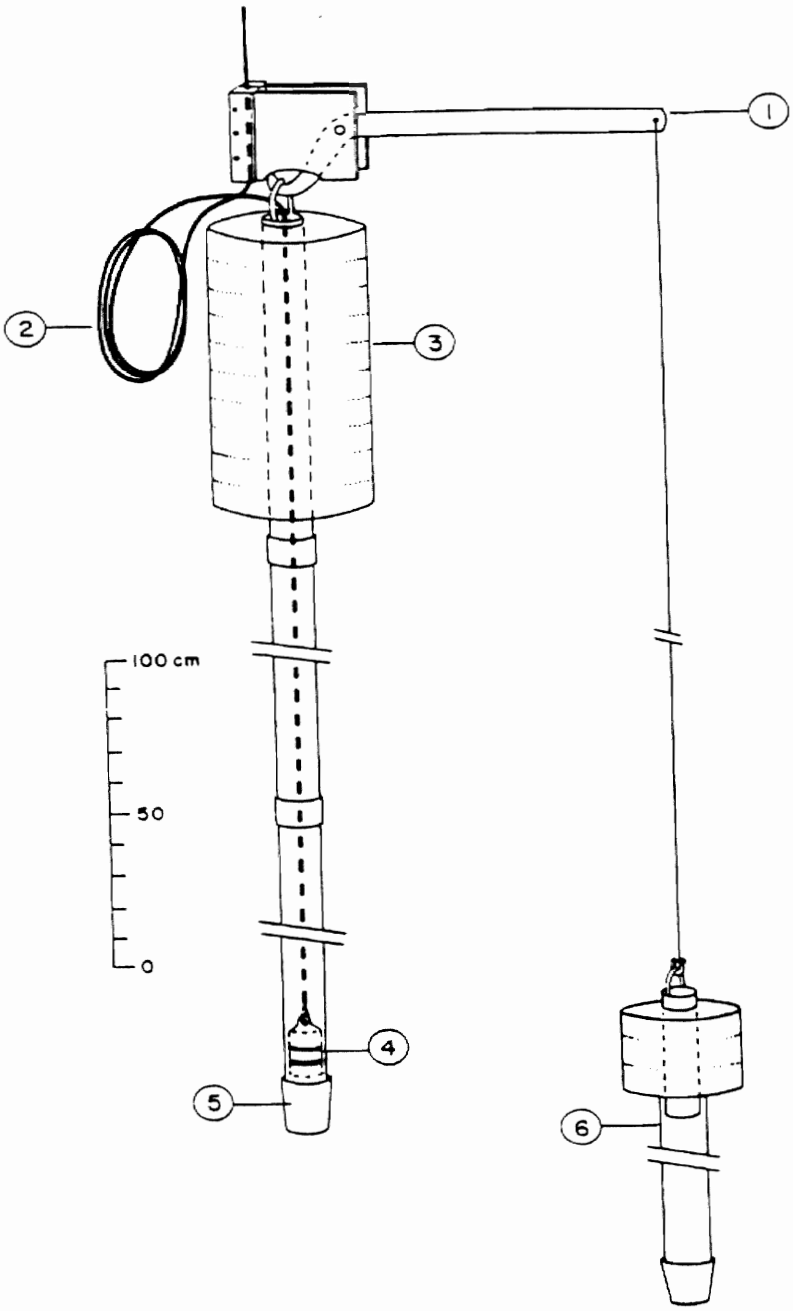

Figure 2.5 Standard Piston Core. 1= Trigger Arm, 2= Wire Loop, 3= Bomb, 4= Piston, 5=Cutter, 6= Trigger Weight Core. (Kennett, 1982)

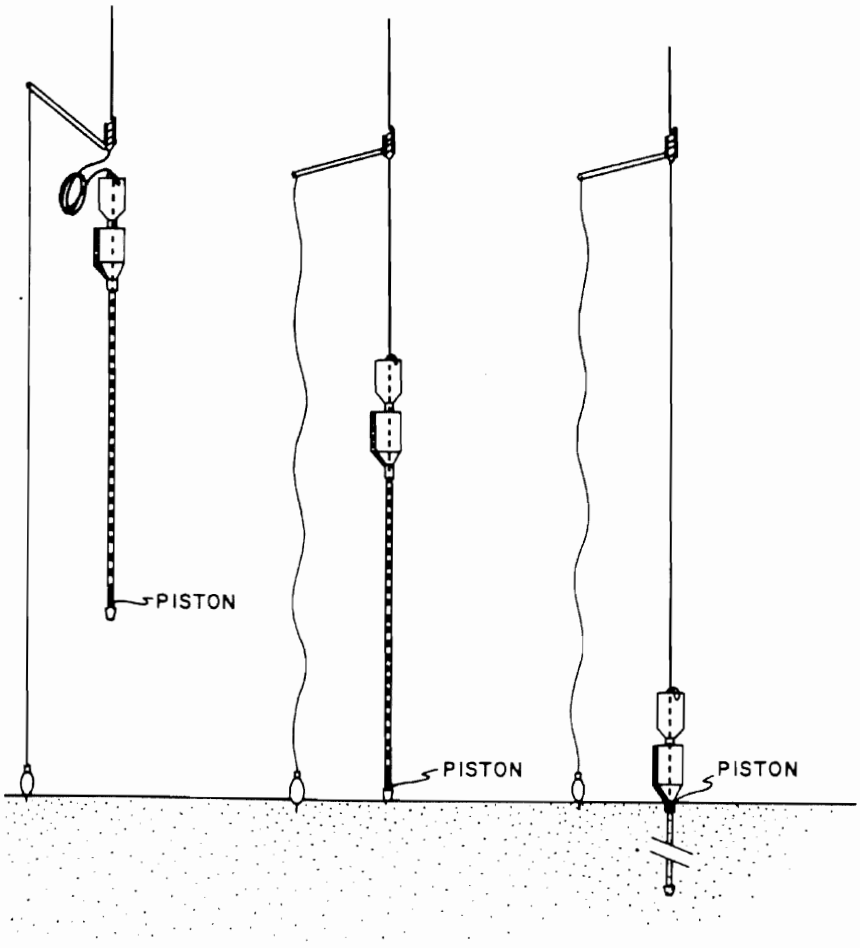

Figure 2.6 Operation of standard piston corer. Calculated wire loop is released at first contact with seafloor, allowing for release and movement of core barrel, for penetration of sediment (Kennett, 1982)

2.5 Standard Lab Procedures

Processing of all cores collected from the study area was done at Bedford Institute of Oceanography (B.I.O.) core lab facility. The whole cores are first passed through the GeoTek Multi-sensor logger which is also referred to as the Multi-sensor Track (MST) The MST measures the following properties; magnetic susceptibility, compressional (P) velocity, and bulk density. The cores are then split longitudinally, with one half labeled

and used as the working half, the other half is stored for undisturbed archive. The archived half is photographed. The working half is used for visual description of sediment color, sediment type, sedimentary structures, fossils, disturbance, etc. The next procedure is to measure color reflectance spectrometry with a hand held Minolta C-2002 spectrophotometer. The results are reported in three numerical values, L representing the black to white, a* represents red to green and the b* representing yellow to black. Discrete measurements of core physical properties are then made, including shear strength, bulk density and acoustic compressional velocity. Discrete measurements of density and velocity provide calibration to the MST data. (Appendix A)

2.6 Seismic data Processing:

Ship board seismic data were recorded in SEG-Y format and then imported into GDMux in-house software, where the Teledyne and Huntec streamer raw seismic lines were concatenated and trimmed into line segments and delay changes were applied. The files were then imported into GEDCO Vista Seismic Processing Software. The data were bandpass filtered, eliminating noise in unwanted frequency bands. A typical bandpass filter frequency range employed for the seismic data was between 35 Hz and 250 Hz. Huntec streamer data were bandpassed between 250 and 2500 Hz. The sea-floor was picked and a static correction was applied to remove sea surface swell effects. Some of the interference noise on the seismic records was removed manually with surgical mute. Subsequently, each line was migrated with a water column velocity of 1500 m/s and an exponential gain recovery was applied from the seafloor to enhance the deepest geological features. The sections were muted to the seafloor and exported as SEG-Y

files. These SEG-Y files were then imported into Seismic-Micro Technologies™ Kingdom Suite interpretation software, where each line was displayed in its appropriate coordinate location (Fig 2.7).

2.7 Seismic Interpretation:

Seismic-Micro Technologies™ Kingdom Suite interpretation software was used to develop the seismic stratigraphy of the study area. Five seismic stratigraphic horizons were defined by key high-amplitude reflectors or noticeable changes in acoustic character. Five key horizons within the study area have been locally correlated with data acquired during Hudson Cruise 2005033B.

Kingdom Suite interpretation software provides three different modes of horizon picking (Table 1.0) of four seismic attributes (Table 1.1). In general, the most effective for high-resolution data was found to be auto-pick fill mode on trace absolute peaks and troughs. This mode allows for manual definition of certain points on a reflection event, between which the computer interpolates a horizon locking to a specified attributes of each seismic trace (White, 2005). Where data were noisy, relative peaks and troughs were picked manually on each trace.

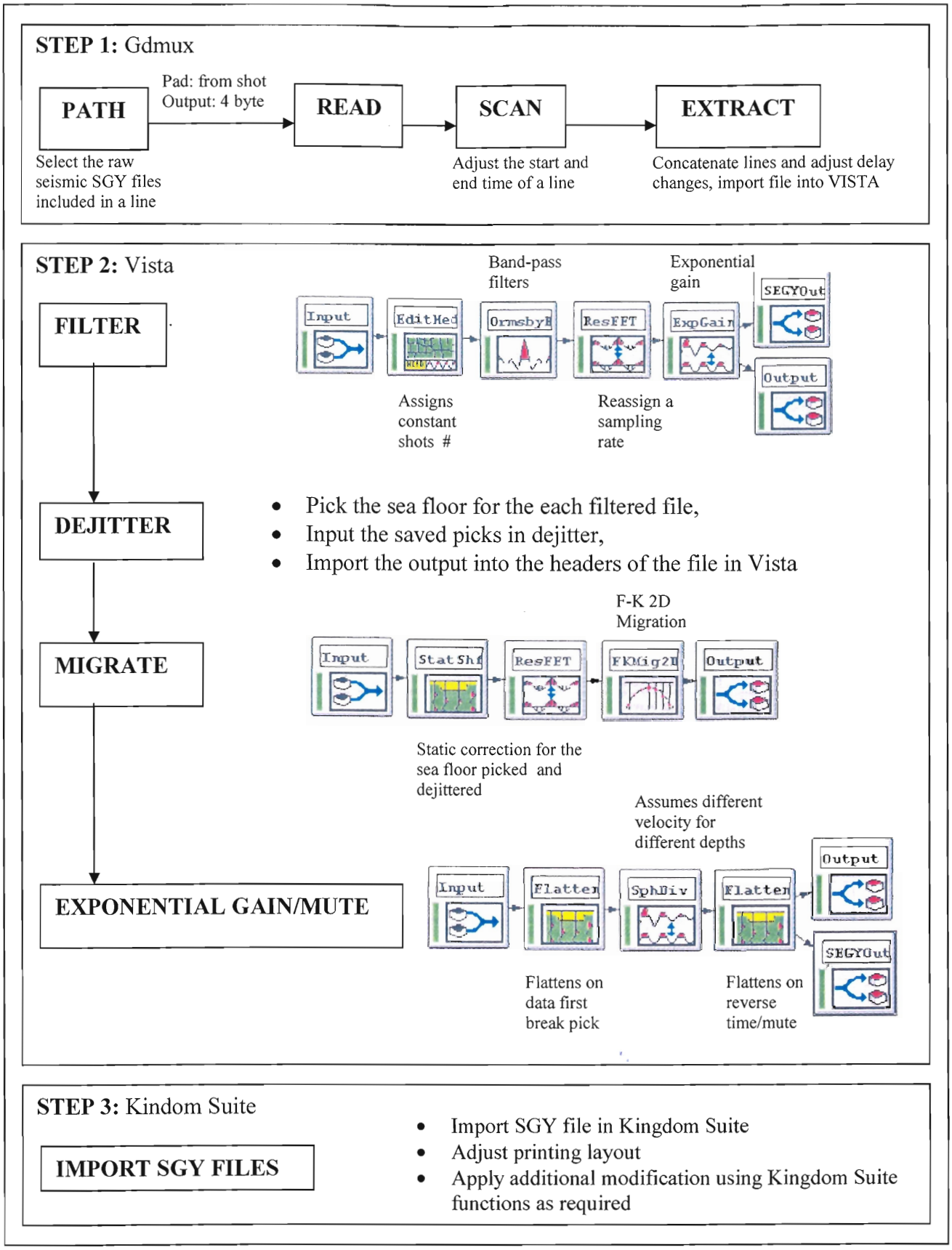

Figure 2.7 Illustrates the workflow for processing the seismic data.

Table 1.0: Picking tools available in Kingdom Suite TKS (Modified after Newton, 2005)

Picking Mode	Description
Manual	Pick points after digitized with single button mouse clicks.
Autopick Fill	Let the autopicker pick between digitized points with the event dropped to the appropriate phase while honoring the guide window. Points are digitized with single button mouse clicks.
Autopick – 2D Hunt	Let the autopicker pick in the left/right direction or both directions from a single click. Picking will stop at the end of an event.

Table 1.1: Methods to pick wave phases provided by Kingdom Suite TKS (Modified after Newton, 2005)

Phase	Description
Peak	A parabola is fit to three samples near the peak. The peak time and amplitude are computed from the parabolic fit.
Trough	A parabola is fit to three samples near the trough. The trough time and amplitude are computed from the parabolic fit.
Zero-crossing (negative to positive)	Time is computed by linear interpolation between negative amplitude and a positive amplitude one sample later.
Zero-crossing (positive to negative)	Time is computed by linear interpolation between positive amplitude and a negative amplitude one sample later.

Chapter 3

Results

3.1 Introduction

Results of the three principle data sources, 1) seismic reflection profiles, 2) Huntec high resolution reflection profiles, and 3) piston cores, are presented in this chapter. Seismic data are described using seismic facies analysis in combination with the seismic stratigraphy established with correlation of five key seismic horizons. Huntec data are also described using seismic facies principles and correlation from core site to core site. Correlation information includes visual descriptions of lithofacies and stratigraphic summary in conjunction with core physical property data.

3.2 Single Channel Seismics

289 km of single channel seismic data were acquired forming the profiles across and along the length of Hamilton Spur.

3.3 Seismic Facies

Seismic facies are defined as portions of seismic data with common acoustic reflection characteristics. These aspects include major external morphologies of seismic features, or the internal reflection attributes (amplitudes, frequencies, and continuity if reflections) (Roger and Noel, 1992). Six different seismic facies were defined within the study area and are illustrated (Fig 3.1). These seismic facies have been distinguished throughout the study area using single channel air gun seismic data and are defined as A-F. Facies A is composed mainly of high amplitude continuous parallel reflectors. This type of acoustic facies is ideal for picking reflectors as they are easily identifiable and can

be correlated locally. The nature of this acoustic facies implies that the associated sediment is well stratified. Facies B is composed of parallel semi-continuous to discontinuous low amplitude reflectors. Facies C is moderately high amplitude chaotic reflectors or mounded stratified reflectors. Facies D is low amplitude discontinuous reflections, as well as acoustically semi-transparent chaotic reflections. Facies E is defined as chaotic reflections of low amplitude that are capped by high amplitude moderately chaotic hummocky reflectors. Facies F are high amplitude, sub-parallel to parallel reflectors; these high amplitude reflectors form large scale sigmoidal structures with asymmetric to symmetric character. Facies F is typically found below facies E.

3.4 Key Reflectors

Five key reflectors have been determined within the study area through mainly single channel seismic air gun profiles (Fig 3.2). These horizons have been correlated within the study with some difficulty because of rapid sediment thickness variations, reflector pinchouts and reflector truncation (Fig 3.2)

3.5 Seismic Units

There are 5 units derived from the 5 key seismic horizons found within the study area. Intervals are described according to their constituent facies and distribution of facies within the intervals. Intervals are referred to by their bounding surfaces; for example blue-magenta interval refers to the area confined between the blue and magenta reflectors. Figures 3.3 and 3.4 show regional down-dip and strike profiles, respectively, which illustrate observations from within the sections. From oldest to youngest, these

sections are: Blue-Magenta, Magenta-Yellow, Yellow-Green, Green-Blue, and Turquoise- Seafloor.

3.5.1 Blue-Magenta Interval

The blue-magenta interval is difficult to resolve as a result of its depth in section and is correlated from the mid to lower slope regions. This interval is composed mainly of facies C. Facies C is generally overlain by facies B in that there is an abundance of low amplitude somewhat stratified reflectors above the high amplitude continuous to discontinuous mounded facies. These high amplitude reflectors are hard to correlate due to the interference of the Huntec DTS signal, even after the signal has been muted from the section. The blue-magenta interval eventually is lost as noise within the data to the west due to signal attenuation with depth. This section thins from mid-slope to the east from approximately 150 ms to 100 ms at the termination of line 50. The strike line implies the same general facies assemblages in which we see facies F, overlain by facies B. This section thickens to the south from 25 ms to approximately 175 ms at the intersection of the down-dip line and strike line, eventually thinning to approximately 80 ms to the far south.

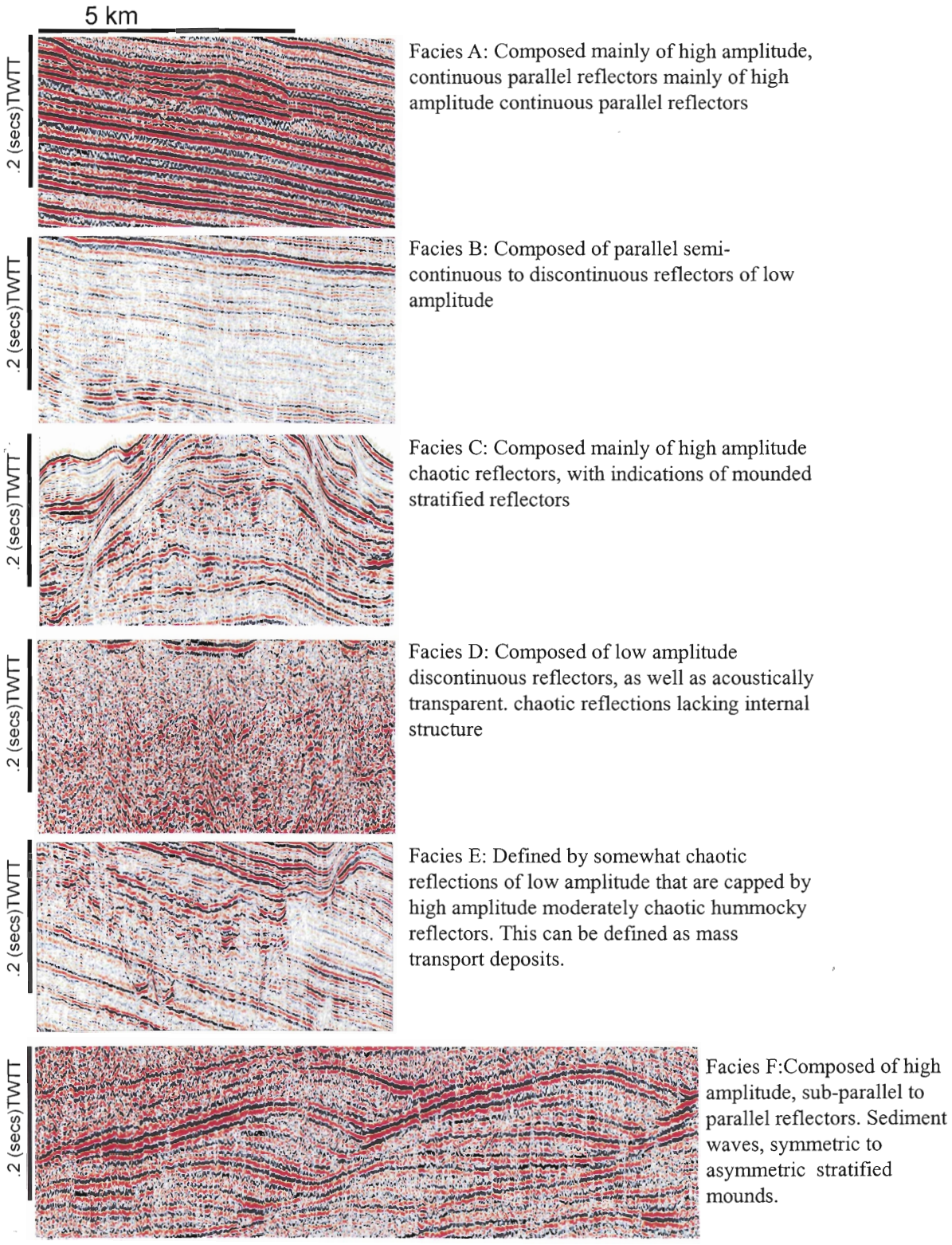

Facies A: Composed mainly of high amplitude, continuous parallel reflectors mainly of high amplitude continuous parallel reflectors

Facies B: Composed of parallel semi-continuous to discontinuous reflectors of low amplitude

Facies C: Composed mainly of high amplitude chaotic reflectors, with indications of mounded stratified reflectors

Facies D: Composed of low amplitude discontinuous reflectors, as well as acoustically transparent. chaotic reflections lacking internal structure

Facies E: Defined by somewhat chaotic reflections of low amplitude that are capped by high amplitude moderately chaotic hummocky reflectors. This can be defined as mass transport deposits.

Facies F:Composed of high amplitude, sub-parallel to parallel reflectors. Sediment waves, symmetric to asymmetric stratified mounds.

Figure 3.1 Six Seismic facies within the study area with corresponding acoustic character. Note that facies are all at the same scale, Two way travel time

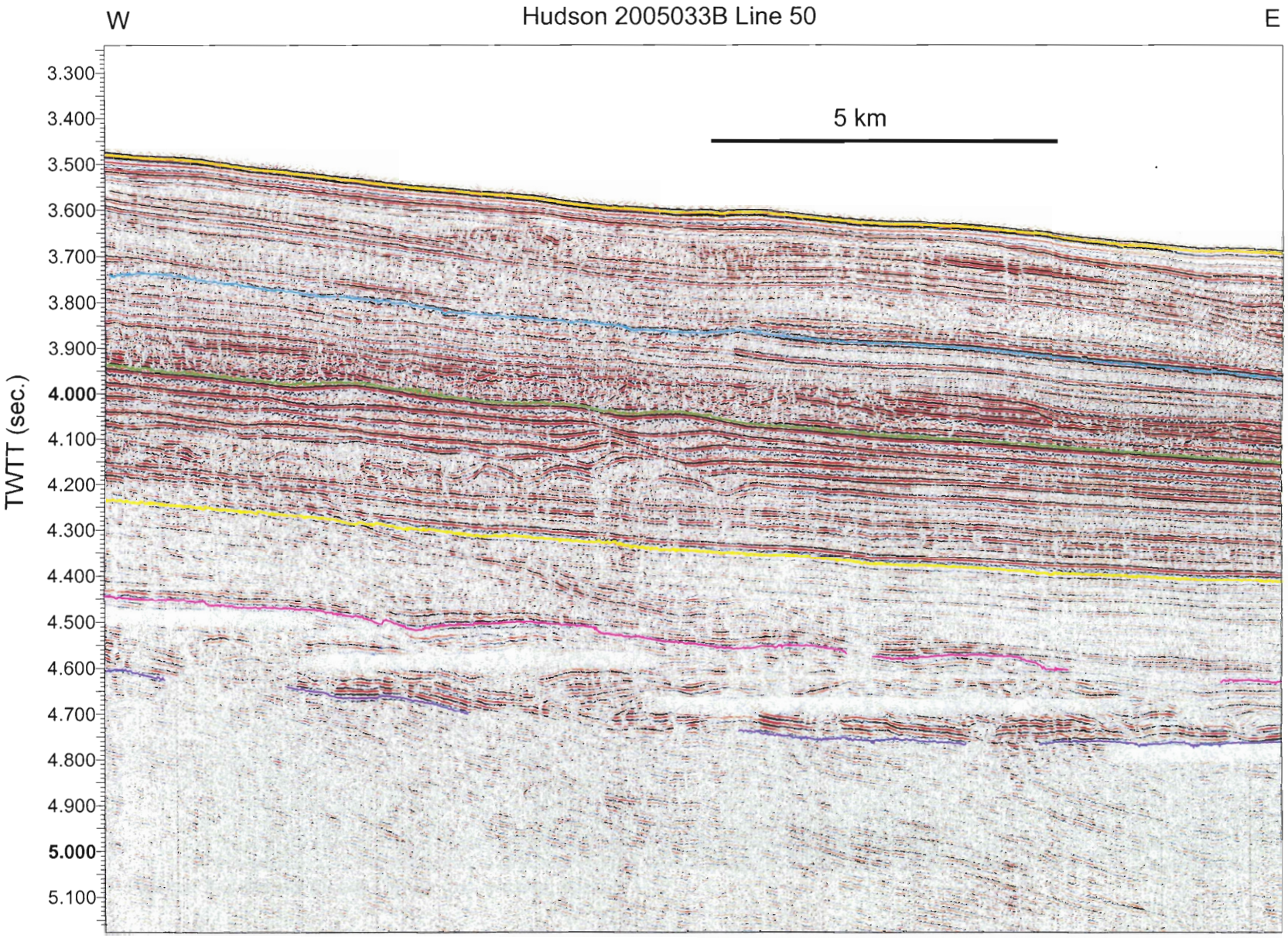

Figure 3.2 Indicates a type section within seismic line 50, in which all 5 horizons are present. The 5 horizons are in order of oldest to youngest; the oldest is identified as blue followed by magenta, yellow, green and turquoise.

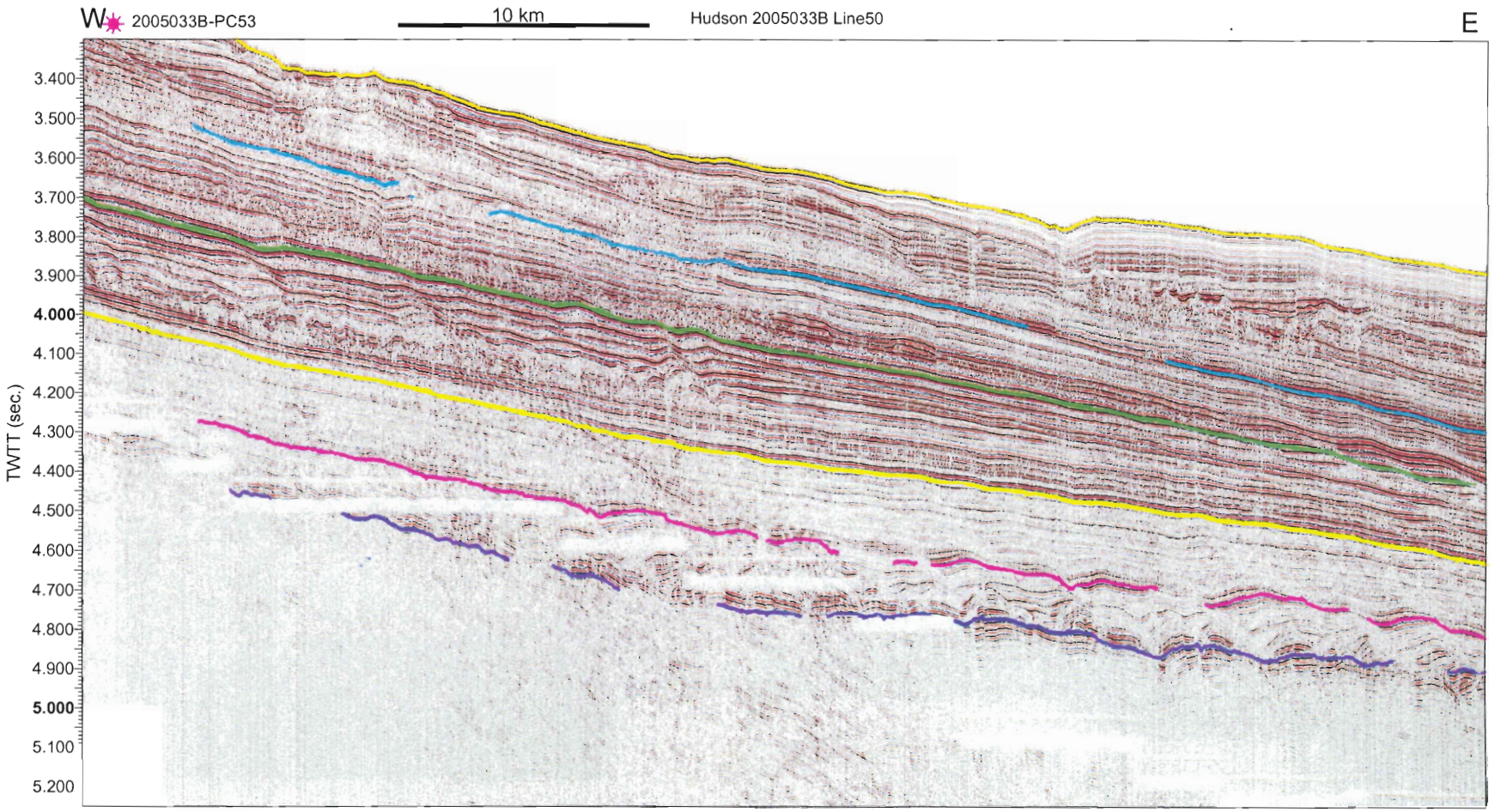

Figure: 3.3 Shows Down-Dip air gun seismic line 50

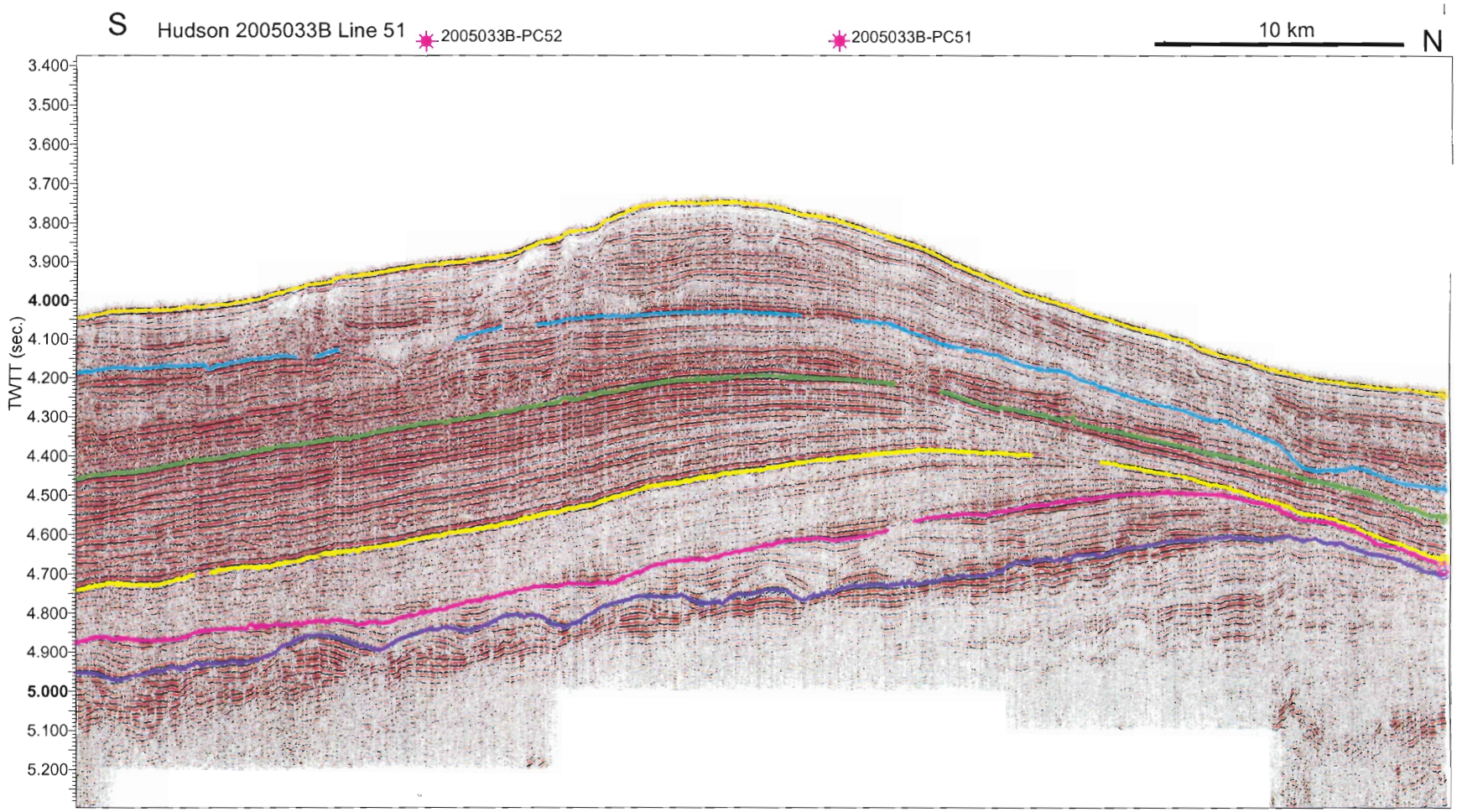

Figure: 3.4 Shows strike section of air gun seismic line 51

3.5.2 Magenta-Yellow Interval

The magenta-yellow interval is composed mainly of facies B; this interval contains almost all continuous low amplitude reflectors, with high amplitude reflectors bounding the interval. The lower third of the magenta-yellow interval consists of low amplitude reflectors which have inherited the characteristics of the large mounded facies located in the interval directly below. This interval seems to keep an average sediment thickness of approximately 200 ms in the down-dip direction. In the strike profile, the same facies pattern is seen but sediment thickness is highly variability with a minimum of 20 ms to the far north, to approximately 200 ms at the intersection of the down-dip and strike lines.

3.5.3 Yellow-Green Interval

The yellow-green interval is composed mainly of facies A and B with minor amounts of facies C and F. Facies A is often underlain by facies B. Facies B is sometimes replaced by facies E, with an abrupt lateral contact between the two facies.

3.5.4 Green-Blue Interval

Within the Green-Blue Interval, three main facies, A, B, and C are noted. Facies F is present within the down-dip section, above the yellow horizon at the upper to mid-slope, facies E lies directly over high amplitude reflectors or even is seen terminating high amplitude reflectors. The chaotic reflectors eventually end down section and the high amplitude reflectors eroded in the upper slope section are found to continue down-dip. These high amplitude reflectors, gradually form facies F, and are found in the lower

slope of the down-dip section. Above facies A, E and F there is a belt of facies B, which are low amplitude parallel reflectors. These reflectors increase in amplitude down-slope.

The Green-Blue interval thins down-slope from approximately 350ms to 120 ms. Along strike, facies E and F are not apparent; only facies present are A and B. Typically facies B overlies facies A, this is seen in particular in the northern end of line 51, working south to the intersection of line 50 and 51. Working south of the intersection of line 50 and 51, facies A is more abundant. Chaotic reflectors disturb the blue horizon over core site 52. The Green-Blue interval thickens from the far north to far south of figure 3.4 from approximately 25 ms sediment thickness, to approximately 220 ms sediment thickness.

3.5.5 Turquoise- Seafloor Interval

The Turquoise-Seafloor interval is separated into three main units: lower, middle and upper. The units are turquoise-middle base unit, middle-upper base unit, and upper to seafloor unit.

Turquoise-middle base unit is composed mainly of facies A and facies B. Facies A generally dominates in abundance and overlies facies B. There are areas within the upper to mid-slope section in which facies E is present, where discontinuous, chaotic reflectors terminate some of the low to medium amplitude reflectors. Facies E is capped by high amplitude reflectors. From the far west to far east of figure 3.3, this unit thins from approximately 200 ms to 100 ms of sediment thickness to the east, down-dip. The strike section appears to have a higher abundance of facies E capped by high amplitude reflectors. There are higher abundances of facies B along strike as well. This unit thins from the intersection of the down-dip line from 100 ms to approximately 50 ms of

sediment thickness (Fig 3.4). To the north of the down-dip and strike intersection, the unit also thins from 100 ms to approximately 30 ms at the northern edge of figure 3.4. Facies C is observed at the intersection of the down-dip and strike line.

The middle-upper base interval within this section is by far the most complicated of all the sections present. There is a large amount of facies B. In down-dip section, in the far west, there is strong evidence of a large channel that cuts down directly from the upper most section. This channel is encompassed by levees which thin away from the channel cut. The channel is almost entirely filled with the uppermost unit, caused by draping or plume fallout which is determined by the presence of high amplitude reflectors of the uppermost unit. The thick strata near the channel levees indicate that there has been deposition of overbank deposits from mass wasting processes. Further down-dip more evidence for channel cuts and facies B are present. Facies A becomes present accompanied by erosional features, followed by facies E, infilling these areas moving down-dip. At the intersection of the down-dip line and strike line, facies C is present within this unit, with large scale complex channel cuts. Facies E completely fills the channels, and is capped by facies A. This unit thins from west to east (figure 3.3) from approximately 250ms to 100ms at the intersection of the strike line. It thickens again due to the complex channel cut and sediment wedging to approximately 200 ms to the furthest east in Figure 3.3. In observing the strike section, further evidence of facies A erosion and in-fill by facies E is apparent. Also found in the southern section of the strike line, and confirmed by Huntec records is the presence of classic shallow gas features. These shallow gas features area accompanied by vertical chimneys, patchy wipeouts with enhanced reflections at the edges, as well as enhanced stratified reflectors. The strike

section appears to thin from the intersection of the down-dip and strike line from 100 ms to approximately 60 ms of sediment thickness at the southern end of the survey line.

The upper-seafloor interval is defined largely by Facies E and A; easily seen in the upper slope regions in the west. There is evidence of large scale evacuation of headwall scarps, which incise into the middle-upper base interval. The evacuation of the headwall scarps, filled the channel within the middle-upper base interval almost completely of high amplitude reflectors. This section thins rapidly from approximately 250 ms to 50 ms sediment thickness down-dip, where it eventually thins enough to become indistinct from the underlying interval, facies A.

3.5.6 Absent Horizons

It is not possible to correlate horizons over the entire spur due to a lack of data, variable geology and data quality. Horizons blue and magenta to the west of the type section (shallower, mid-slope regions) on seismic air gun line 50 become absent laterally due to lack of seismic penetration (Figure 3.3). Although termination occurs to the west for magenta and blue horizons, they are easily correlated to the east on line 50 (Figs. 3.3 & 3.4), as well as north and south on seismic air gun line 51, seen in Figure 3.4. Seismic air gun lines 53 and 54 continue to the west from seismic air gun line 51, in mid to upper slope regions where two horizons green and blue are able to be correlated. With data presented in the above sections, it is worth noting that green and blue are the only two horizons within the seismic air gun data that are correlated throughout the entire study area.

3.6 Huntec DTS Seismics

Huntec DTS seismic data were collected simultaneously with the air gun data. The Huntec system provides high definition profile images of shallower reflectors. The data were digital processed over core sites 51, 52 and 53 (Figures 3.5, 3.6, 3.7) and for other selected sections. Otherwise, the data acquired shipboard in real time were used for interpretation and core to core correlation. The use of Huntec DTS data were useful to tie in shallower stratigraphy with the three piston cores collected, in the hope to get approximate age dates from shallow reflectors.

3.7 Huntec Reflectors

There are 6 reflectors within Huntec data that have been defined, denoted as R1-R6; R6 being the oldest at greatest depth and R1 being the youngest at shallowest depths. Within Figures 3.5, 3.6, 3.7, the location of each core has been established. The cores are depicted as white lines at scale on the sections, allowing for stratigraphic correlation between cores, Huntec DTS data, as well as air gun seismic data.

Huntec DTS seismic data at core site 51 (Fig 3.7) show high amplitude reflectors R1-R4 seen within core penetration depth. Below core penetration depth, the presence of two more high amplitude reflectors (R5-R6) are distinguished. Reflector R6 is oldest of the six reflectors and lies approximately at 80 ms sub-bottom depth. This 80 ms sub bottom marker can also be seen on air gun seismic line 50 profile between the blue-seafloor interval within the middle unit.

Correlation has been made between core sites 51 and 52, using digital and analog paper records. At core sight 52 (Fig 3.6), reflectors R1-R4 have correlated directly from core site 51. Reflectors R1-R3 are seen in core, while location of reflectors R4-R6 are

seen below core penetration depth due to increasing sediment thickness along-strike. Correlation of reflectors R5 and R6 presented a challenge due to the Huntec penetration threshold; probable locations of reflectors R5 and R6 have only be assumed (Fig 3.6).

Correlation to core site 53 (Fig 3.7) was done tracing reflectors back to site 51, down-dip. In core site 53 reflectors R2-R3 have been positively correlated and are seen within core penetration depth, R1 is faint and cannot be correlated. As well, correlation was easily made with reflectors R4-R5, which lie below the penetration depth of the piston core, but are above the threshold limit for Huntec data capability. Reflector R6 could not be correlated because it presumably lies below the Huntec depth limit (Fig 3.7).

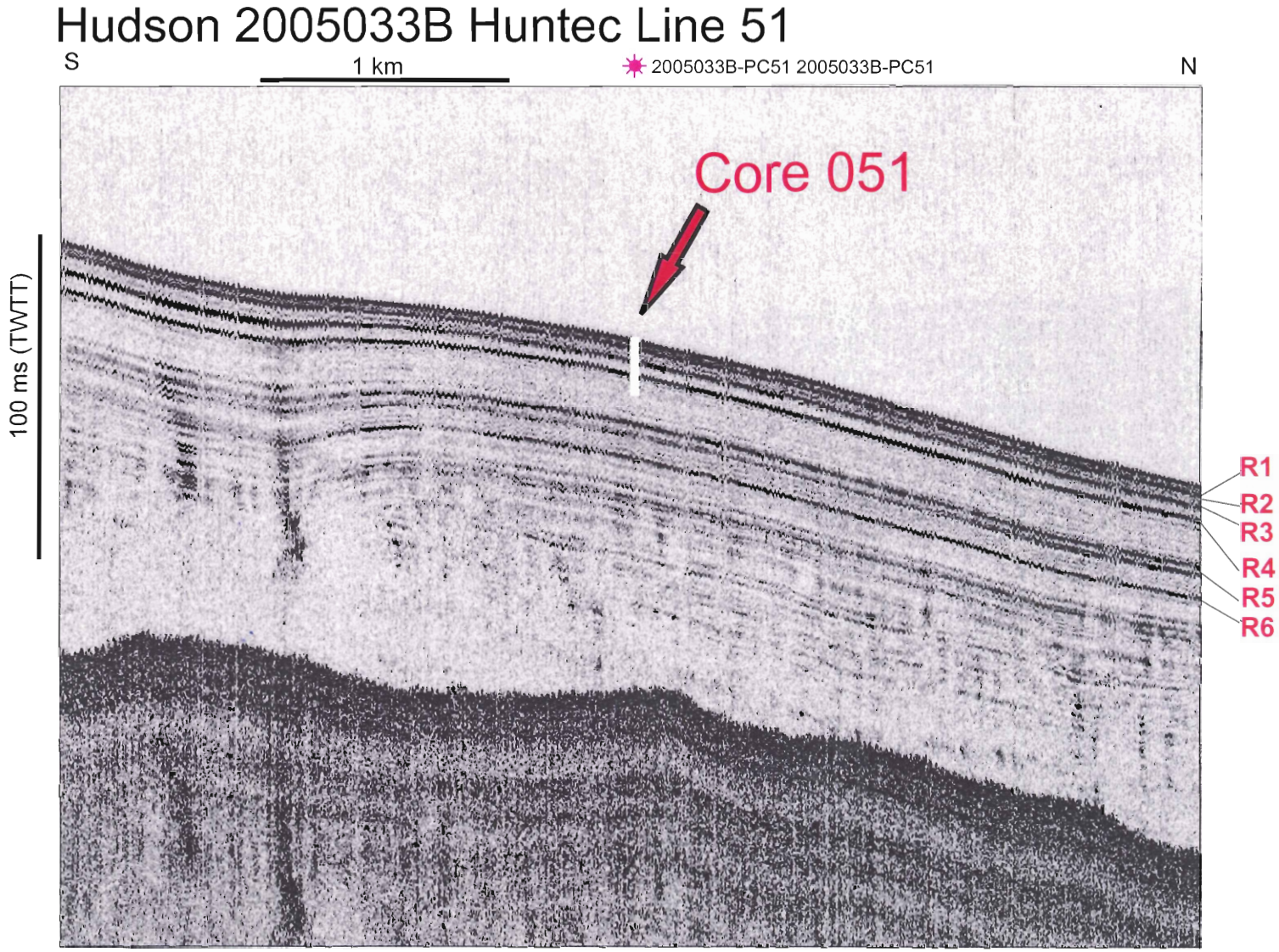

Figure 3.5 Indicating location of piston core 51, and locations of key reflectors

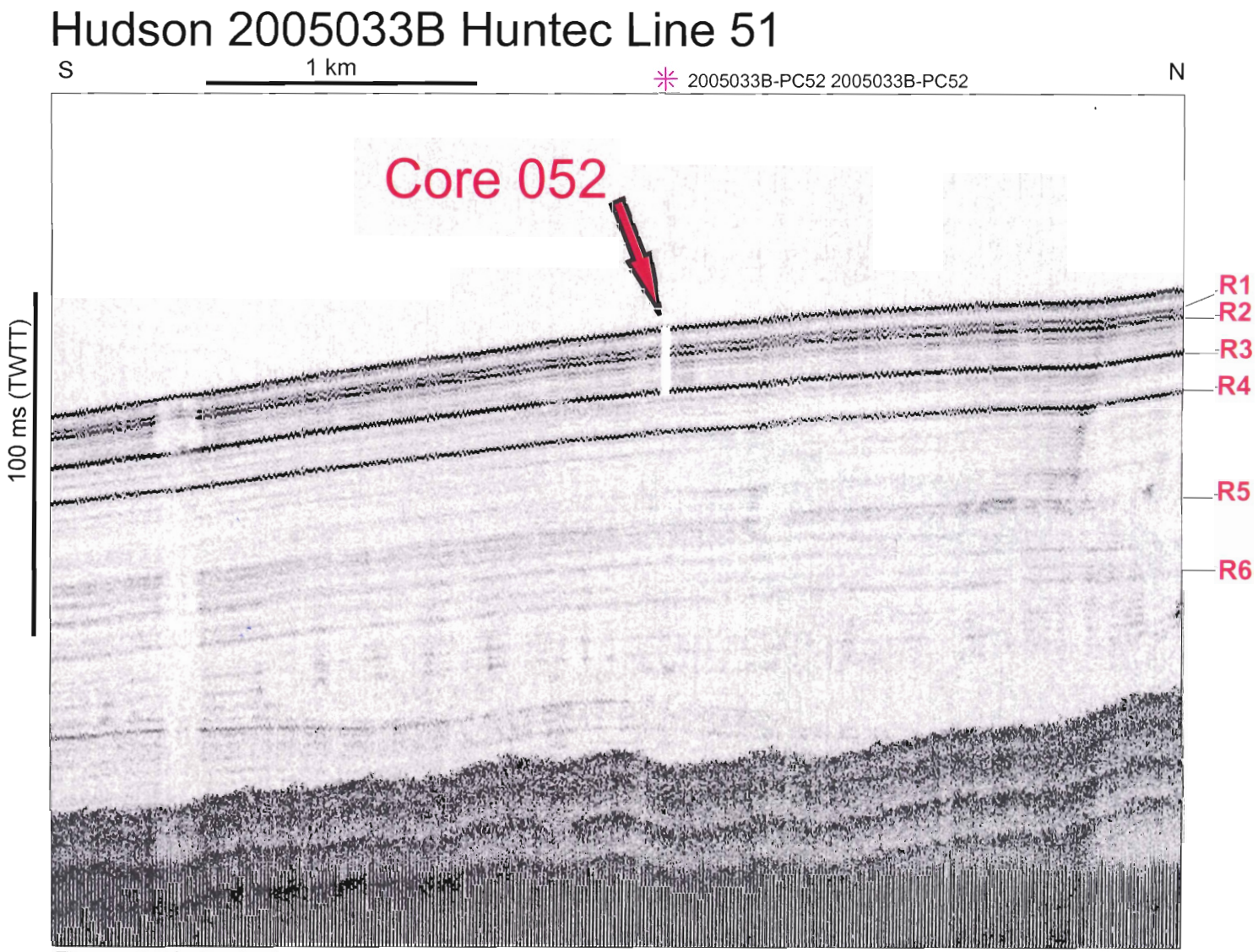

Figure 3.6 Indicates location of piston core 52, and location of key reflectors.

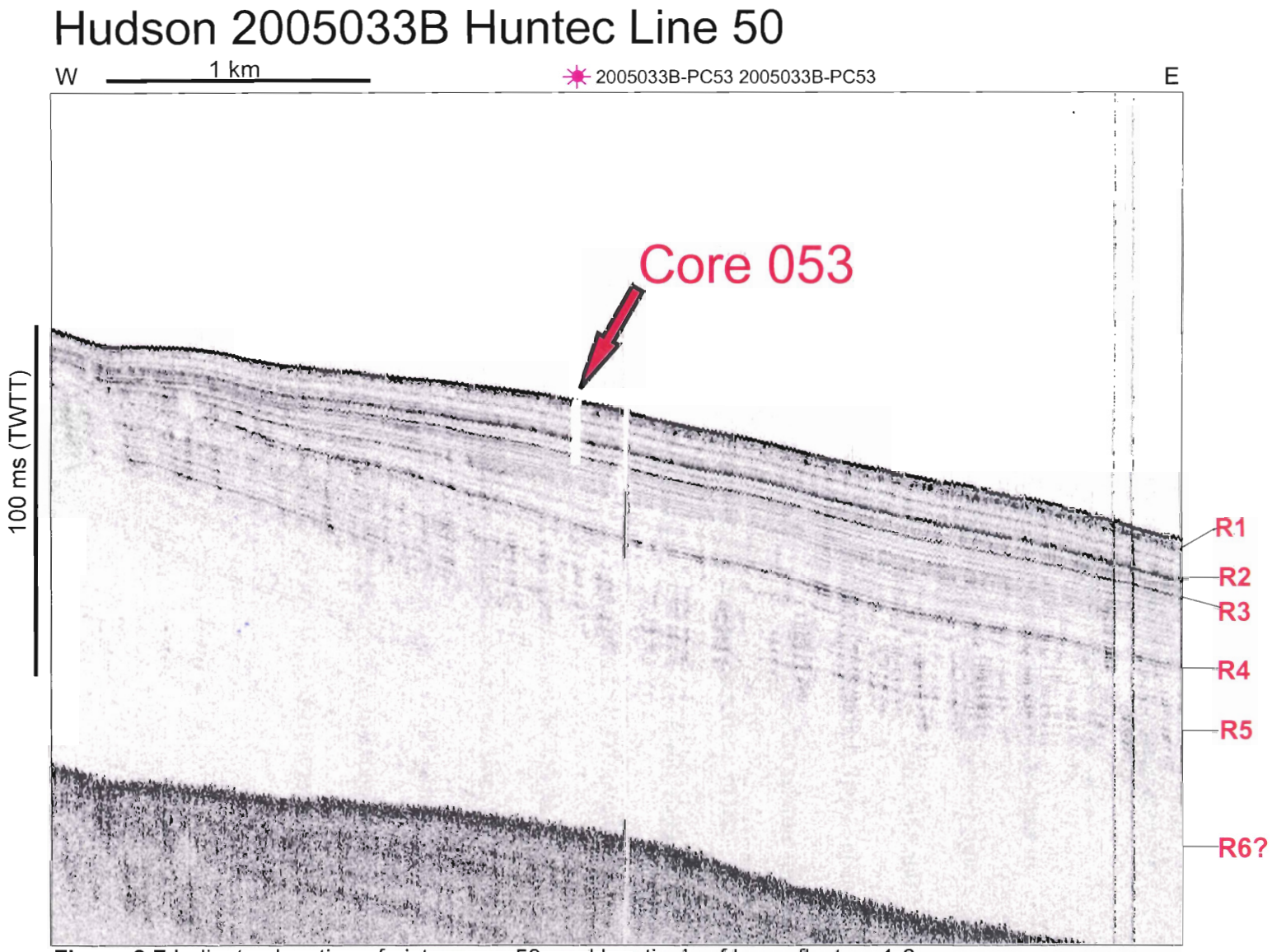

Figure 3.7 Indicates location of piston core 53, and location's of key reflectors 1-6.

3.8 Piston Cores

Three piston cores (051, 052 and 053) were acquired within the study area on Hamilton Spur during mission Huds2005033B. The purpose for these cores is to understand Late Pleistocene to Holocene sedimentation patterns on Hamilton Spur in order to determine glacial and deep current influences and their interactions over time. Locations for cores 051, 052, and 053 are shown in Figures 2.1 and 3.8. Cores 051 and 052 are located on seismic line 51 striking NNW-SSE across the Hamilton Spur. Seismic line 50 trends east-west down-slope of Hamilton Spurs ridge and intersects seismic line 51. Core 51 is located to the north of this intersection, on the northern flank of the Hamilton Spur (55.04° latitude and 51.32° longitude) in 2734 m water depth. Core 052 lies on the southern flank of the Hamilton Spur (54.65° latitude and 51.24° longitude) in 2902 m water depth, located south of the intersection of seismic lines 50 and 51. Core 053 lies on seismic line 50, to the east of the intersection point of seismic lines 50 and 51. Core 053 is located on the down-slope ridge of the Hamilton Spur (54.52° latitude and 52.00° longitude) in 2351 m water depth. Locations were determined in expectation of seeing variations in Labrador Current and Western Boundary Undercurrent influences at three key locations.

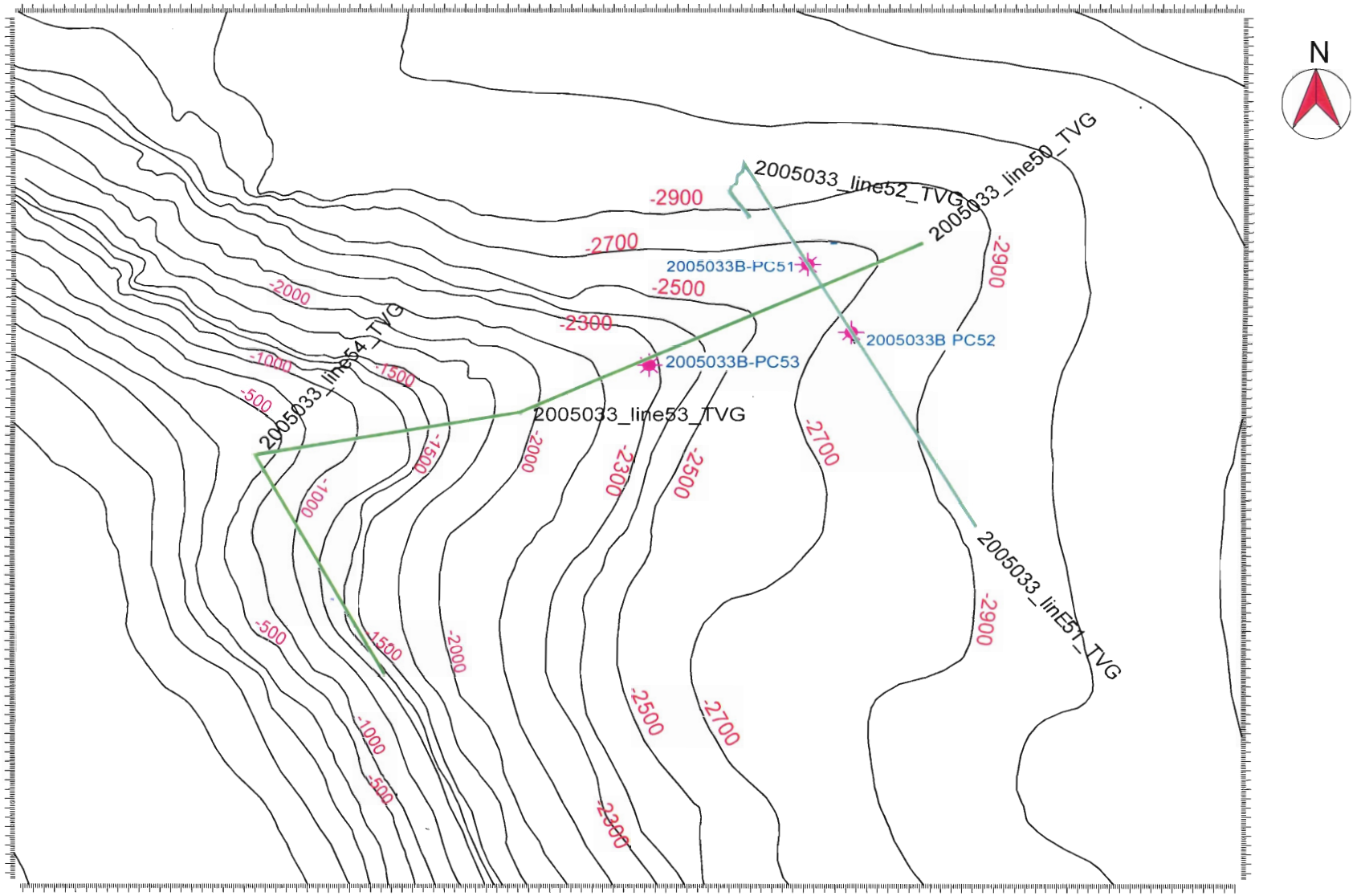

Figure 3.8 Indicating locations of core sites 051, 052, and 053

3.8.1 Lithofacies

In the three cores studied off the Hamilton Spur, comprising 41m of core, 5 distinct lithofacies were recognized. These five distinct facies for this study are classified as: Facies I: Olive silty-sandy clays, Facies II: Olive grey silty-sandy clays with ice rafted debris (IRD), Facies: III: Tan silty-sandy clays, Facies IV: Brown (reddish) silty-sandy clays and Facies V: Green grayish silty-sandy clays. Figure 3.9 shows facies distribution and appendix A contains physical properties measurements).

Facies I

Facies I consists of Olive silty sands and clays. Facies I is common within all three cores and is found to be deposited below facies II, in the mid to lower sections of the cores. Facies I has gradational contacts with Facies II, IV, V, but forms sharp distinct contacts with Facies III. This particular facies is massive, void of burrows, and structures. Physical properties such as magnetic susceptibility and density of Faces I are distinct from the four remaining facies

Facies II

Facies II comprises the majority of the 41 m of core collected, found mostly in the upper and mid sections of core facies II commonly bounds facies III, and overlies facies I. Bounding surfaces between facies II and III are sharp and distinct, and typically gradational with facies I, IV, and V. Facies II consists of mainly olive grey silty-sandy clays with occasional ice rafted debris (IRD). Not uncommon are numerous clasts, granules, burrows, and disseminated sands found throughout the facies. Other key characteristics of facies II are the fine laminations, forams and moderate degrees of mottling.

Facies III is the most visually distinctive facies found throughout the upper to mid sections of cores, particularly cores 051, and 052. Facies III consists of tan-colored silty sands and clays, with occasional clasts and pebbles. Facies III has sharp contacts with the overlying and underlying facies. Physical properties of facies III are distinct with high values of velocity, density, and L, a* and b* color spectrums.

Facies IV is found minimally throughout the 41 m of core. It is visually distinct with thin laminations throughout. Facies IV forms sharp contacts with facies III, and gradational contacts with facies I, II, and V. Little variability is found in physical properties of Facies IV, but there is a small amount of moderate peaking found within the L color values.

Facies V consist of mainly grayish green silty-sands and clays and is found in the mid to lower sections of the cores, especially that of cores 052, and 053. This facies is massive and forms gradational contacts with facies I, II, and IV. There is little variation in physical properties that distinguishes this facies, a magnetic susceptibly increase is the only noticeable characteristic.

Facies Associations in Piston Cores 051, 052, 053

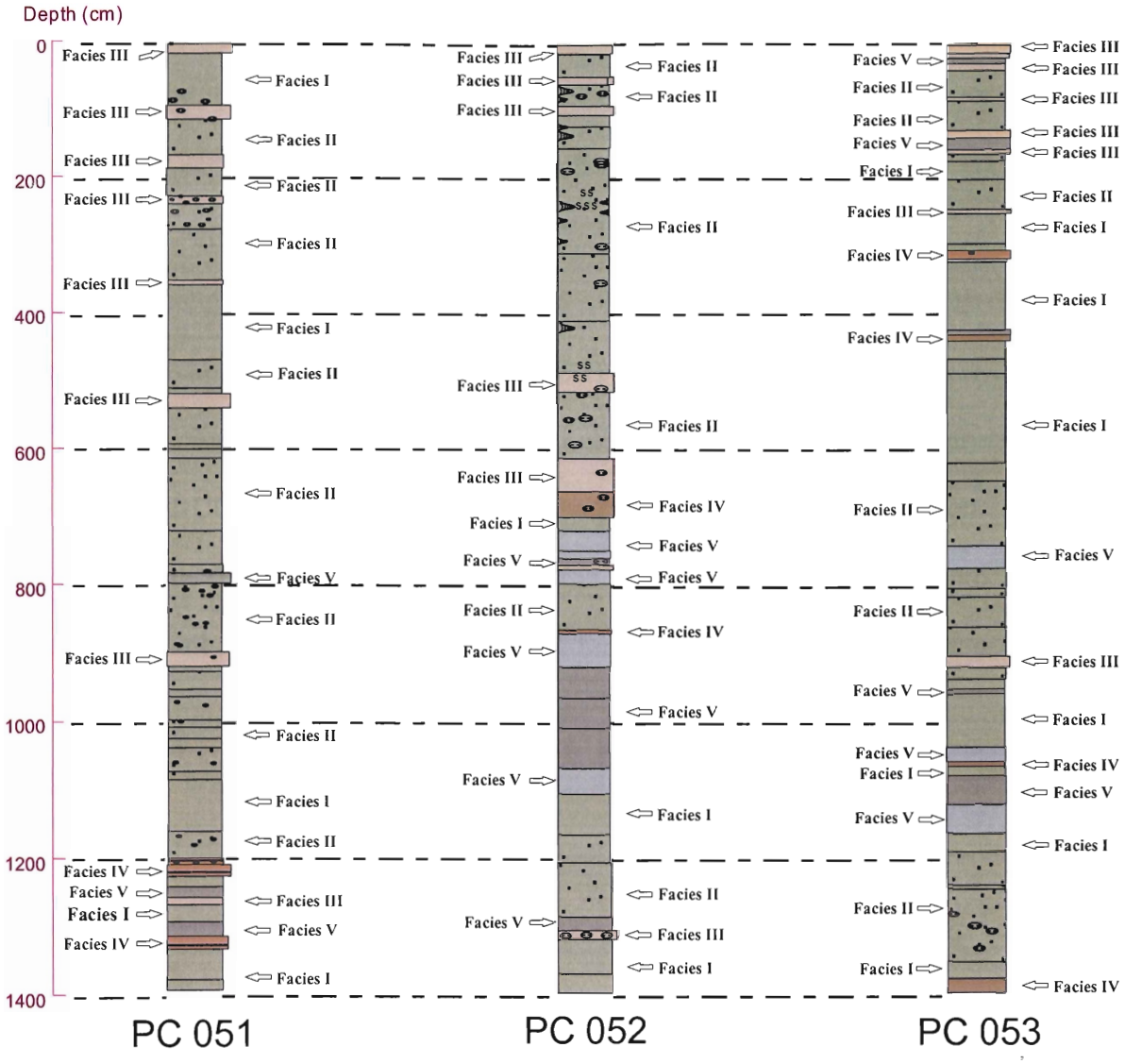

Facies I: Olive grey silty-sandy clays

Facies II: Olive grey silty-sandy clays with IRD

Facies III: Tan silty-sandy clays
Brown (reddish) silty-sandy clays

Facies IV:

Facies V: Green grayish-brown silty-sandy clays.

Figure 3.9 Facies Associations on Piston Cores 051,052,and 053

Chapter 4

Discussion and conclusions

The Hamilton Spur is a large scale drift deposit forming in the early Cenozoic (Myers et al. 1988), located in the southwest Labrador Sea between 300 m and 3000 m water depth at approximately 55° N, and 54° W. The Hamilton Spur is a major topographic feature of the Labrador continental margin formed by the interaction of the Labrador Current (LC) and the Western Boundary Undercurrent (WBUC). These currents are responsible for reworking and depositing continental margin sediments. Presently, the LC and the WBUC are considered the two major driving forces of sedimentation processes on the flanks and ridge of the Hamilton Spur, although depositional processes such as slope failure, are additional factors. Within this chapter, evidence of intense southward flowing current from both the LC and WBUC is provided. Previous work done on the LC and WBUC, in conjunction with seismic data, Huntec data and three piston cores collected for this study allows for the determination of the stratigraphic evolution and morphological history of the Hamilton Spur.

4.1 Labrador Current and Western Boundary Undercurrent

The Labrador margin is swept by two southward flowing currents, the LC and the WBUC. The LC flows southward on the Labrador margin's upper slope regions, while the WBUC is present at greater depths on the lower slope and rise. There is a separation of these two southward flowing currents defined by a "zone of no motion" located at approximately 1200 m water depth (Figure 4.1, 4.2). These currents are generated by the direct result of sea-water stratification, in which dense water from the Scotland-Iceland-

Greenland regions sink. The Coriolis effect forces the LC and WBUC currents to the west where bathymetric highs force flow to the south and/or obliquely up-slope. (Carter et al, 1983). Velocity measurements conducted on the WBUC presented by Rabinowitz & Eittreim (1974), and Allen & Huntley (1977) indicate that north of the study area the mean current velocity is approximately 12 cm sec^{-1} east of Hopedale Saddle at 3000 mbsl. South of the Hopedale Saddle there is a bend in topography where contours trending approximately northwest at 340° abruptly change to 290° northwest. This 50° change in contour direction causes redirection and intensification in current velocity from 12 cm sec^{-1} to 20 cm sec^{-1} to just south of the Hamilton Spur ridge where there is a decline in velocity to approximately 10 cm sec^{-1}. Similarly, data have been collected for the LC in which mean velocities reach as high as 30 cm sec^{-1} (Carter et al, 1983). These velocity measurements of undercurrents show that the undercurrents are capable of winnowing out mud. Data presented in Carter et al, 1982, suggest that the WBUC has a high speed core at approximately 2800 m. At this depth, the sediments are coarsest, and display the maximum development of current structure (Carter et al, 1983). This observation is directly related to this study in which both cores 051 and 052 lie at approximately 2800 m depth, and depict similar results with high abundance of coarser sediments and sediment bedding than that of core 053 at approximately 2300 m depth, consisting of more massive material.

Labrador Current & Western Boundary Undercurrent

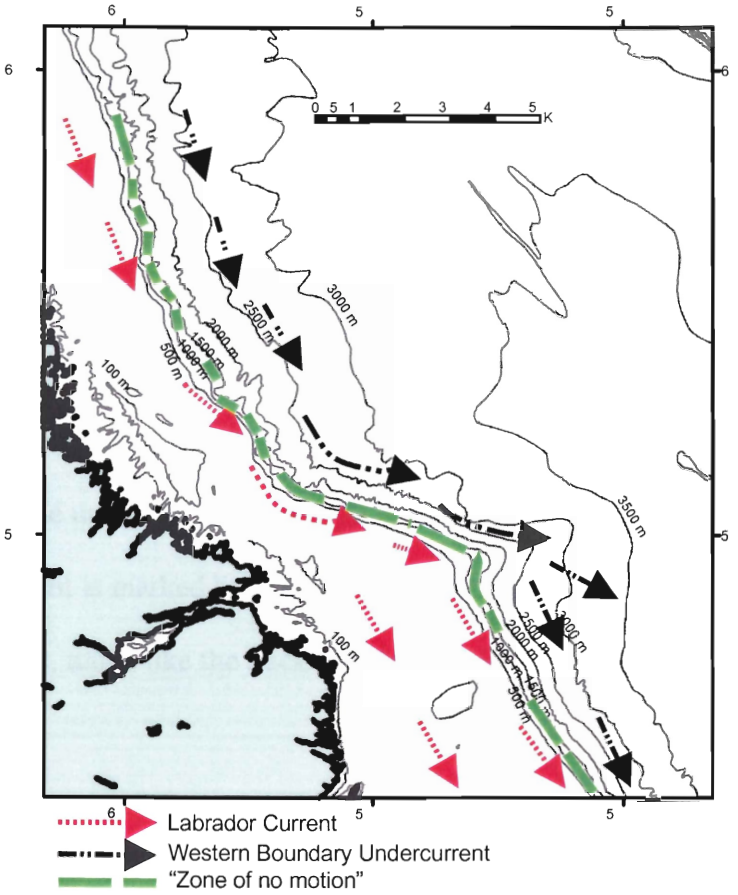

Figure 4.1 Diagram indicating projected pathways of the LC and WBUC

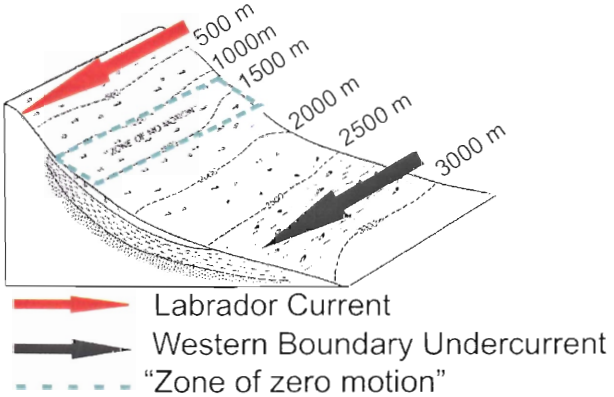

Figure 4.2 Cross-section diagram of LC and WBUC locations

4.2 Assessment of Single Channel Air Gun Seismic Data

Results of the single channel seismic data indicate current-influenced deposition, directly associated with bottom-current reworking of the deeper offshore components of the LC, and the underlying WBUC, since the late Pliocene to early Pleistocene. To the north and south of Hamilton Spur, there are thick deposits found beneath the Labrador Rise. Reflector packages thin rapidly towards the continental slope, and a major near surface unconformity is present above 2000 m depth on the continental slope (e.g. Figs. 3.2, 3.3, and 3.4 indicate the unconformity underlying the Blue interval). The initiation of the deep LC flow component is marked by this large scale unconformity distinctive near the base of the drift deposit, much like the Sackville Spur to the south (Kennard et al, 1990)

Above the unconformity, there are 5 intervals in which different seismic facies have been defined. Within these intervals, individual reflector horizons are hard to correlate due to erosion, reflector termination, sediment mounding, and on-lapping of thick continental rise deposits. Seismic line 51 (Fig 3.4), across Hamilton Spur in water depths greater then 2600 m, shows the development of a well stratified asymmetric mound. This mound forms the present day spur in these water depths. Underlying the northern flank of the present day spur ridge, at greater depths, is a similar looking mounded deposit, indicating there was southward movement of the spur's depocenter. This observation is also seen in (Fig 3.4), in which each interval between the Blue and Seafloor reflectors, experience thickening to the south from the present day ridge crest on the southern flanks.

Sediment waves are present at the base of the Blue-Magenta interval directly above the unconformity, (Fig 3.3 & 3.4). These sediment waves have truncated the underlying strata, indicating that in places bottom current activity eroded the southern Labrador Slope. This fact indicates a change in erosional to depositional conditions, which leads to the assumption that there was a decrease in current velocity. The Blue-Magenta interval mimics these sediment waves throughout the interval to the base of the Magenta-Yellow interval.

The Magenta-Yellow interval has low amplitude continuous reflectors that in down-dip section maintain thickness throughout (Fig 3.3) to the extreme west and east, but show thickening in the southern direction from the ridge crest to the far south (Fig 3.4). This observation implies a relatively consistent pattern of current flow across the length of the spur but reduction in velocity on the lee (southern) side with concomitant sediment deposition.

The Yellow-Green interval is noticeably different than the underlying one, with numerous well-stratified reflectors (Fig 3.3 & 3.4). Facies A bright reflectors may be indicative of intensification of bottom water flows, leading to coarser-grained sedimentation and establishment of strong bedding. Facies B may represent deposition from less intense current flow, perhaps even suspension settling.

There is evidence of mass transport deposits (MTD) in this interval where reflectors of facies B are truncated by vertical contacts with facies E. High amplitude reflectors frequently cap these facies E occurrences. The chaotic reflection pattern of facies E is interpreted to represent sediment mass flow and the capping reflector is a consequence of a sharp impedance contrast with overlying sediment. Deep currents acting on the surface of the MTD may leave a coarse lag.

The Yellow-Green interval averages a constant thickness of approximately 300 ms down-dip. The strike section shows almost the same facies configuration but lacks facies C and F within the extent of the seismic section

The Green-Blue interval is dominated mainly by high amplitude reflectors of facies A, as well as chaotic reflectors. Typically facies E, overlies the high amplitude reflectors where the termination of these high amplitude reflectors is seen. It is interpreted that the high amplitude reflectors were truncated by mass transport deposits. Erosional and draping reflection patterns are common in this interval, possibly indicative of periods of current intensification.

The uppermost interval, Blue-Seafloor, consists of three units. Present in the lowermost units are chaotic reflectors truncating low to medium amplitude reflectors. This interval likely represents MTD's. Hummocky stratified facies within this interval are the direct result of slumping and draping, overlying strata are seen mimicking these structures.

Wavy-stratified seismic facies in the Blue to Seafloor interval are possibly contourite bedforms. On the northern flanks, the presence of wavy-stratified mounds are interpreted as contourite build-up below 2800 m water depth. At the sea-bed, smaller asymmetric and symmetric sediment waves have been determined to be formed by the direct result of bottom currents. The distribution of these sediment waves at depths around 2800 m probably marks the axis of the strongest WBUC.

To the west, on the outer shelf and upper slope above the sediment wave region, high amplitude reflectors are cut by gullies, creating mound and levee like features. Buried channel-like features are also present within this interval, typically found on the rise. The orientation of these channel features is not known. It is more likely that they

represent downslope flowing currents, such as turbidity currents than contour parallel currents.

4.3 Huntec Deep Tow Data Assessment

Huntec data, which is higher resolution then the air gun data and shows greater detail in the upper ~100 m of sediment reveals that the LC and WBUC influence modern sedimentation patterns across Hamilton Spur. Huntec data show six main high amplitude reflectors within the top ~20 m sub-seafloor. These reflectors intersect core sites (051, 052 and 053) at various depths, often within the depth of core penetration.

Core site 51 is located on the northern flank of the Hamilton Spur in 2734 m water depth just shallow of the WBUC main axis. Core 051 contains all 6 reflectors (R1-R6). R1 and R2 are approximately 0.02 ms TWTT (Two Way Travel Time) apart, followed by a 0.05 ms TWTT difference separating R2-R3 and R3 and R4. The R4-R5 interval is much greater with a TWTT distance of 0.12 ms and the R5-R6 interval is less then the overlying interval at 0.05 ms TWTT.

Core site 052 on the southern flank of the spur, in 2902 m water depth, shows evidence of thickening in all intervals. Here, R1 and R2 have clear spacing between them of approximately 0.05 ms TWTT. Intervals R2-R3 and R3-R4 maintain a uniform separation similar to site 051 with a TWTT of 0.10 ms. As well the R4-R5 interval has increased to approximately 0.025 ms TWTT and the R5-R6 interval has increased to approximately 0.20 ms TWTT.

The correlation between cores 051 and 052 has been done by comparing the shallow Huntec reflectors as well as the physical properties measurements for the two cores. Huntec records indicate that there are 3 strong reflectors present in both core 051

and 052. These strong reflectors have been interpreted to be Heinrich events and are important correlation horizons. As described above and seen in the Huntec profiles (Fig 3.5 & 3.6) there is thickening of sediments from the north to south. Thicknesses between R1 to R3 reflectors present in core 051 become approximately twice that in core 052. Correlation was first made by tracing these reflectors from site 051 to 052 on Huntec analog paper records. Next the core lithofacies descriptions (Fig 3.9) and physical properties (appendix A) of each core were compared revealing similar properties between the R1-R3 reflectors. Physical properties such as velocity, density and color allow for correlation of reflectors by matching patterns in data peaks and troughs. Positive correlation of reflectors R1-R3 supports the observations in Huntec data that there has been substantial sediment deposition on the southern flanks, and of current reworking of the northern flank at 2800 m.

Huntec correlation from core site 51 to 52 is straight forward as reflectors R1-R6 are present and correlateable along line 51. Core site 053 lies on seismic line 50, in 2350 m water depth, on the main ridge of the Hamilton Spur. Here evidence of the LC and WBUC interactions becoming more defined and sequence thicknesses are distinct from the other sites. At core site 053, R2-R5 are positively correlated from core site 051, reflectors R1 and R6 could not be distinguished. Correlation between core 051 and 053 has been done only with reflector R2 using the Huntec records and physical properties measurements as described earlier for correlation of 051 and 052. While correlating the analog Huntec records from core 051, the location of reflector R1 becomes uncertain due to possible winnowing of R1 by bottom current reworking at the time of deposition or soon after. Physical property data and lithologies, as well, show an absence of R1 in core 053. Seismic signal attenuation has been determined as the explanation for the absence of

reflector R6 at site 053. Overall, the shallow sequence thickens significantly at site 053, particularly within the R3 to R4 interval. This increase in sediment thickness at the shallowest site implies that deep water current activity is more intense at 2800 m than 2300 m. This observation confirms the observations of Carter et al. (1983), with the core of the WBUC lying at about 2800 m water depth.

There is definite thickening of sediments on the southern flank of the Hamilton Spur over that of the northern flank. In correlating cores 051 and 052 there is thickening of all the intervals R1-R6 (figure 4.3), in almost every interval sediment thickness has increased by two fold from site 051 to 052. This fact is likely a result of the southward propagation of the WBUC, with bottom current intensification on the stoss (northern) side of the spur, and less on the leeward (southern flank), leading to higher sedimentation rates on the lee.

Textural characteristics of sediments in cores 051 and 052 also suggest the WBUC as the driving force for sedimentation, with higher amounts of fine sands, and lesser amounts of silt. Core site 053 mainly consisting of winnowed silts and clay sized particles suggests that the main sediment driving force is the upper WBUC.

Correlation of Piston Cores 051, 052, 053

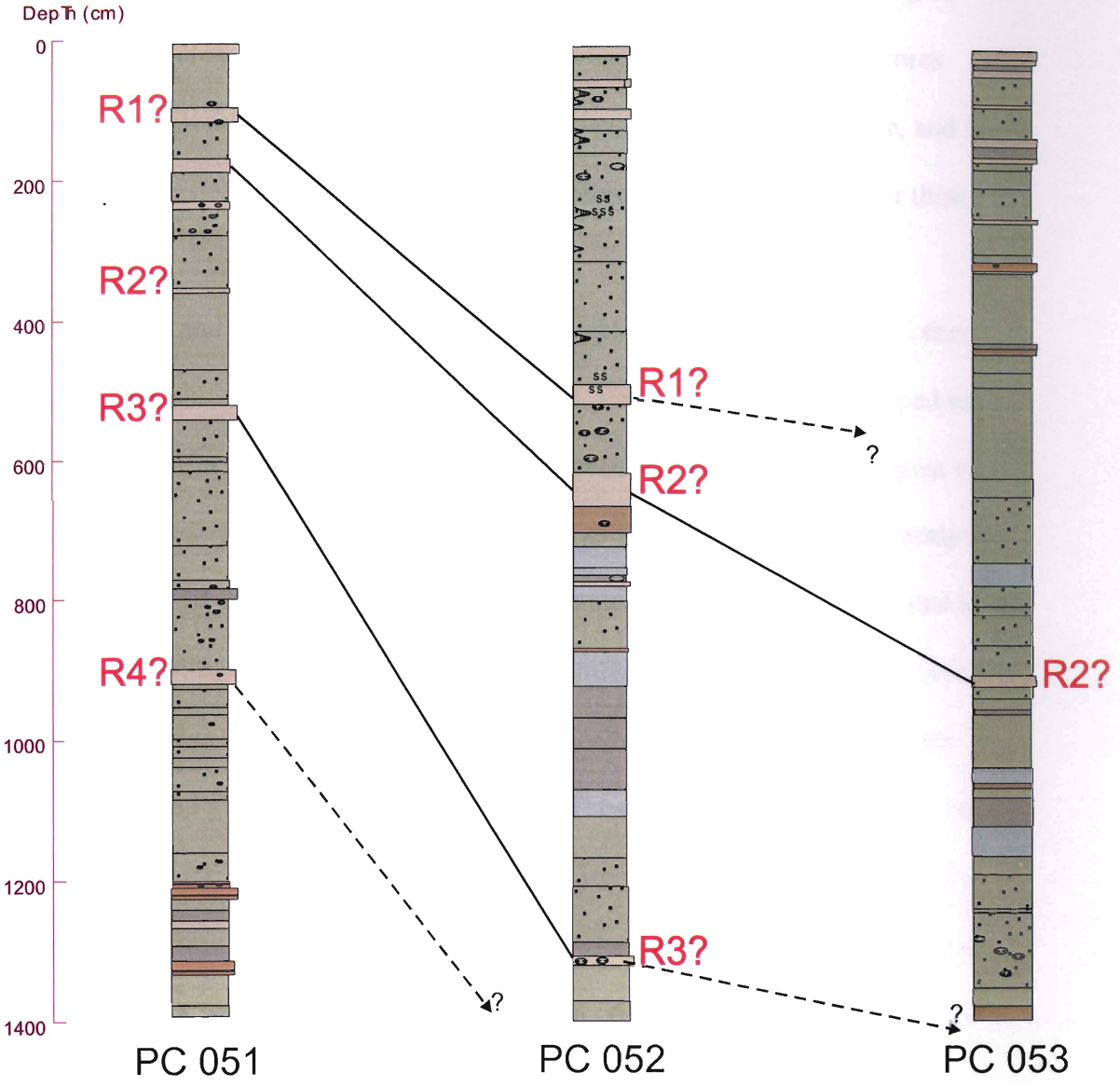

Facies I: Olive grey silty-sandy clays

Facies II: Olive grey silty-sandy clays with IRD

Facies III: Tan silty-sandy clays

Facies IV: Brown (reddish) silty-sandy clays

Facies V: Green grayish-brown silty-sandy clays.

Figure 4.3 Indicates probable correlation of piston cores 051, 052, and 053

4.4 Analysis of cores 051, 052, and 053

Cores recovered were used to help define the shallow stratigraphy, and give insight to textural characteristics, color, and transport analysis. As well these cores support the ideas on how the currents interact from west to east down the ridge, and north to south across the spur. There are presently no absolute-age dates available for these cores.

In textural and stratigraphic analyses, Cores 051 and 052 resemble each other remarkably, each showing a similar pattern of facies. Facies generally are grouped in packages in which facies II, overlies facies III, followed by facies I, where a repeat in the pattern occurs. These patterns are indicative of change in depositional environments and conditions. Facies III is the most recognizable, presumed to be Heinrich events that form distinct contacts with overlying and underlying sediment. These events aid correlation of facies, cores, and ties to Huntec records. The presence of presumed Heinrich events reflects wide-spread glaciations in the Quaternary. These Heinrich events are the result of glacier melt as the ice retreated northward towards Greenland (Kennard et al, 1990). Sediments at this time were deposited from melting glaciers creating thick blankets of glacial material. As well, these glaciers caused a reduction in bottom water circulation at times of glaciations directly effecting sediment reworking.

It is interpreted throughout the eastern North American margin that most of the sediment delivery occurred during glacial recessions (Myers et al, 1988). On the continental margin slopes, the principal delivery mechanism is believed to be from turbidity flows as grounded ice sheets on the shelves caused a progradation of sediment from the shelf to the northwestern canyons. Turbidity flows created "spill-over" deposits which were suspended within the current and deposited after crossing the ridge crest from

the less intense southward flowing currents. This leads to the conclusion that most of the spur was built during the Plio-Pleistocene times when sediment delivery due to glaciation was maximum.

4.5 Why did the Spur form initially at this location?

Hamilton Spur likely formed under bathymetric control of deep currents such as the LC and WBUC. Sharply bending contours east of the Hopedale saddle allowed the LC and WBUC intensity to increase. The presence of canyons to the northwest of the Hamilton Spur allowed for "spillover" sediments from turbidity flows to be carried in the currents to the ridge of the Hamilton Spur. These sediments were likely deposited as current intensity decreased over the ridge. As well, these strong currents in the deeper regions are capable of bottom reworking and re-suspension. These sediments were again deposited just over the ridge of the spur where current velocity is diminished. Once the Hamilton Spur was established, its own shape further modifies current conditions, which controls its continuing evolution.

4.6 Conclusions

The Hamilton Spur is a prominent feature of Labrador Sea. This large sediment drift formed mainly in the Pliocene-Pleistocene by the interactions of the southward flowing Labrador Current and Western Boundary Undercurrent, with the underlying topography. Its stratigraphic succession provides some clues to its formation and evolution.

The initiation of the Labrador Current and Western Boundary Undercurrent presumably eroded a pre-existing drift deposit causing the creation of an angular

unconformity. Canyons present in the topography to the northwest of the Spur are responsible for turbidity "spill-over" sediments to be suspended and deposited over the spur's ridge. Strong bottom currents are also responsible for the reworking and eroding material on the northern flanks and ridge of the Hamilton Spur. Sedimentation was enhanced due to glacial retreats causing blankets of glacial debris to be deposited. Heinrich Events within the cores provide evidence to the occurrence of glacial episodes and that sediment within the cores is glacially-derived. Slumping and mass wasting processes to the northwest contribute to today's building of the Hamilton Spur. Sediment cores and ultra high-resolution seismic profiles show that the Hamilton Spur depocenter today still maintains its southward movement under the influence of both the Labrador Current and the Western Boundary Undercurrent.

4.7 Recommendations for Further Work

There is a paucity of data for the Labrador margin and the surrounding regions, but particularly on Hamilton Spur. As hydrocarbon exploration proceeds to the Labrador margin and in ever deeper water, there is a need for better understanding of the Labrador Seas stratigraphy and deep water sedimentary processes. Future work could be separated into categories 1) Air gun seismics and Huntec Seismics 2) Further core analysis (radiocarbon dating, isotope dating, sediment size, properties, and distribution), 3) Current study (intensity measurements, etc) and 4) Glacial history. Once sufficient data has been worked up on the study area, it could be compared to similar type drifts (Sackville Spur and Orphan Spur) which may help understand the processes and distributions of these large scale sediment drifts.

List of References:

Balkwill, H.R., McMillan, N.J., MacLean, B., Williams, G.L., and Srivastava, S.P. 1990. Geology of the Labrador Shelf, Baffin Bay, and Davis Strait., Chapter 7, in Geology of the Continental Margin of Eastern Canada, M.J., Keen and G.L. Williams (ed.); Geological Survey of Canada, Geology of Canada, no. 2, p-293-348 (also Geological Society of America, The geology of North America, v. I-1).

Caddah, L.F.G., Kowsmannn, R.O., Viana, A.R., 1998. Slope sedimentary facies associated with Pleistocene and Holocene sea-level changes, Campos Basin, southeast Brazilian Margin. Sedimentary Geology, v. 115, p. 159-174.

Carter, L., and Schafer C. T., 1983. Interaction of the Western Boundary Undercurrent with the continental margin offshore Newfoundland. Sedimentology. v. 30. p. 751-768

Carter, L., Schafer, C.T., and Rashid, M., 1979. Observations on depositional environments and benthos of the continental slope and rise, east of Newfoundland. Canadian Journal of Earth Sciences, v.16. p. 831-846

Chough, S.K., Mosher, D.C., and Srivastava, S.P. 1985. Ocean Drilling Program (ODP) site survey (Hudson 84-030) in the Labrador Sea: 3.5 kHz profiles; in current Research, part B, Geological Society of Canada, Paper 85-1B, p. 33-41.

Faugeres J.C., Mezerais, L.M., and Stow, D.A.V. 1993. Contourite drift types and their distribution in the North and Sourth Atlantic Ocean basins. Sedimentary Geology, v. 82, p. 189-203

Faugeres, J.C., and Stow D.A.V., 1993. Bottom-current-controlled sedimentation: a synthesis of the contourite problem. Sedimentary Geology. v. 82. p. 287-297

Josenhans, H.W. and Barrie, J.V., 1989. Submersible observations on the Labrador Shelf and Hudson Strait; in Submersible observations off the East Coast of Canada, D.J.W. Piper, editor; Geological Survey of Canada Paper, p. 88-20, 41-56.

Kennard, L., Schafer, C., and Carter, L., 1990. Late Cenozoic evolution of Sackville Spur: a sediment drift on the Newfoundland continental slope. Canadian Journal of Earth Sciences. v. 27, p. 863-878

Kennett, J. P., 1982. Marine Geology. Prentice-Hall Inc., p. 95-96

Mosher, D.C., 2005. CCGS Hudson Cruise 2005-033 B expedition report, Grand Banks, Orphan Basin and Labrador Sea, Unpublished GSC Internal Report.

Myers, R.A. and Piper, D. J.W., 1988. Seismic Stratigraphy of late Cenozoic sediments in the northern Labrador Sea; a history of bottom current circulation and glaciation. Canadian Journal of Earth Sciences. v. 25, p. 2059-2074

Rashid, H., Hesse, R., and Piper, D.J.W., 2003. Evidence for an additional Heinrich event between H5 and H6 in the Labrador Sea, Paleoceanography, v. 18, p.1077, doi:10. 1029/2003Pa000913

Rashid, H., Hesse, R., and Piper, D.J.W., 2003. Origin of unusually thick Heinrich layers in ice-proximal regions of the northwest Labrador Sea, Earth and Planetary Science, Letters v. 208, p. 319-336

Srivastava, S. P., and Roest, W.R., 1999. Extent of oceanic crust in the Labrador Sea. Marine and Petroleum Geology. v. 16, p. 65-84

Swallow, J. C and Worthington, L.V. 1969. Deep Currents in the Labrador Sea. Deep-sea Res, v.16, p. 77-84.

Viana, R.A., 2002. Seismic expression of shallow- to deep water contourites along the south-eastern Brazilian Margin. Marine Geophysical Researches, v. 22, p 509-521.

Walker, R.G. and James, N.P. 1992. Facies Models, Response to sea-level change. Geological Assoication of Canada. Series IV.

White, M.C. 2005. Late Cenozoic Seismic Stratigraphy of the Mohican Channel Area, Scotian Slope. B.Sc. thesis, Dalhousie University, Halifax, Nova Scotia.

Appendix A: Physical Properties for Cores 051, 052, 053

Hudson 2005033B PC 051

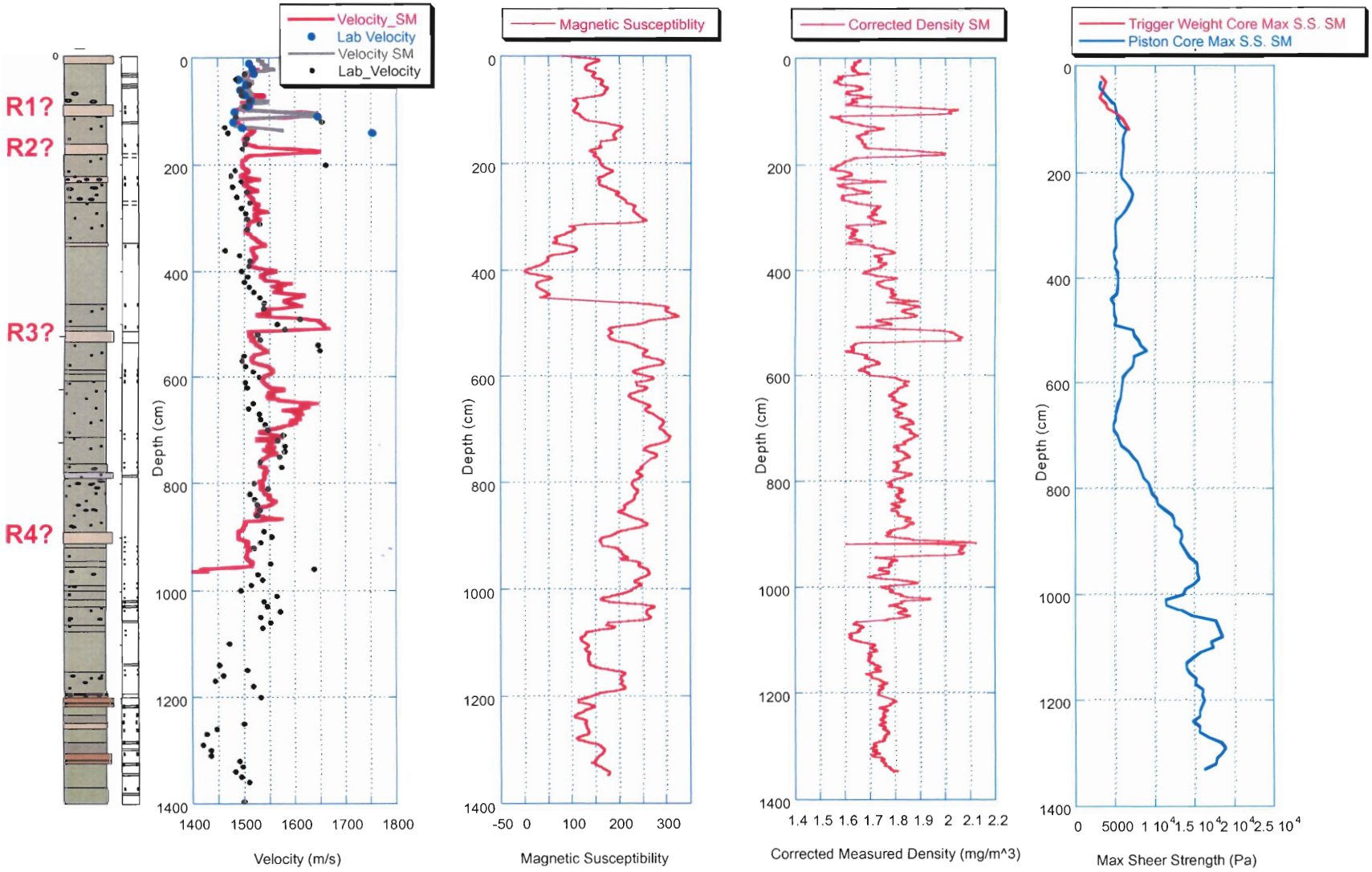

Hudson 2005033B PC 052

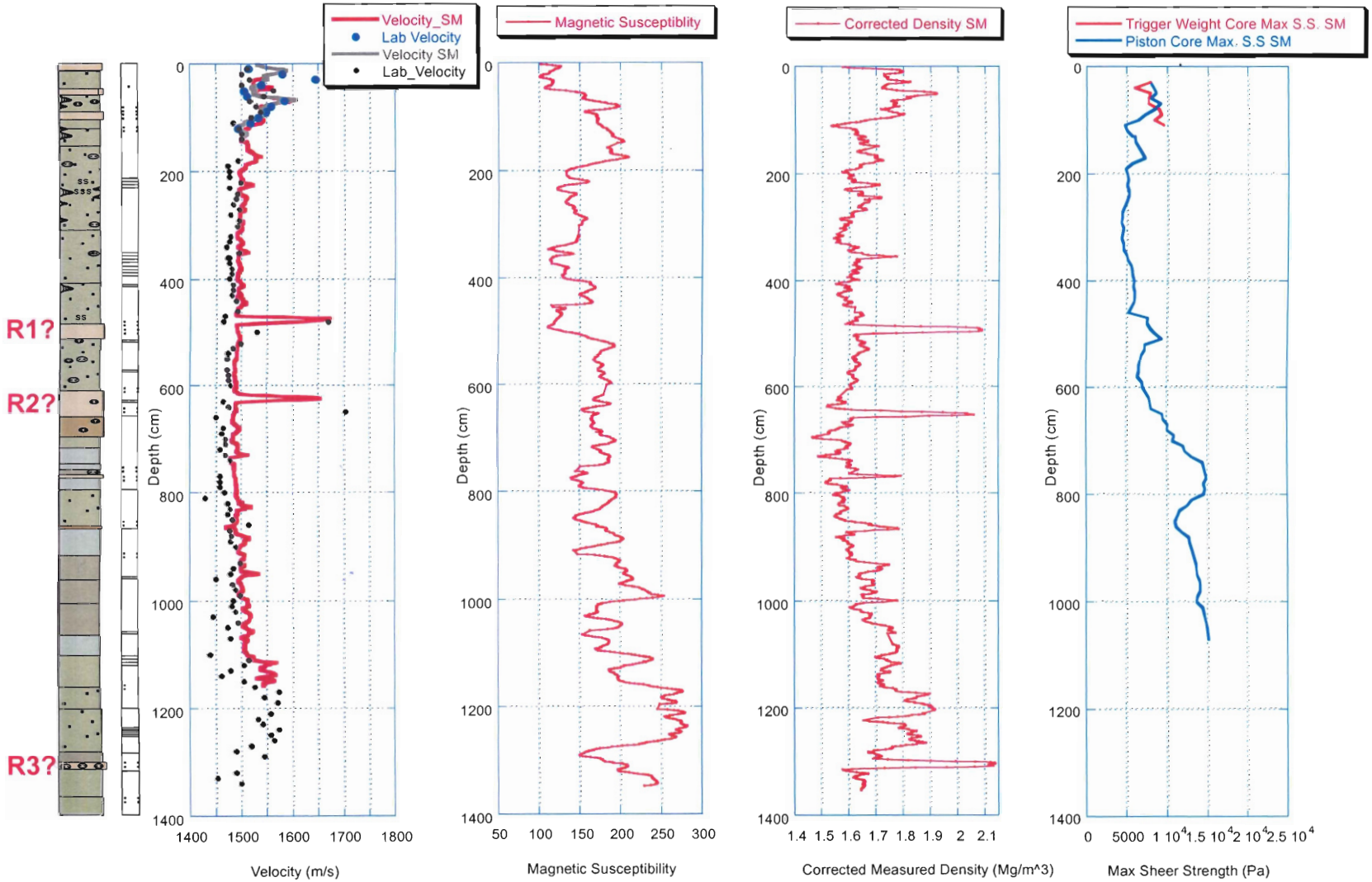

Hudson 2005033B PC 053

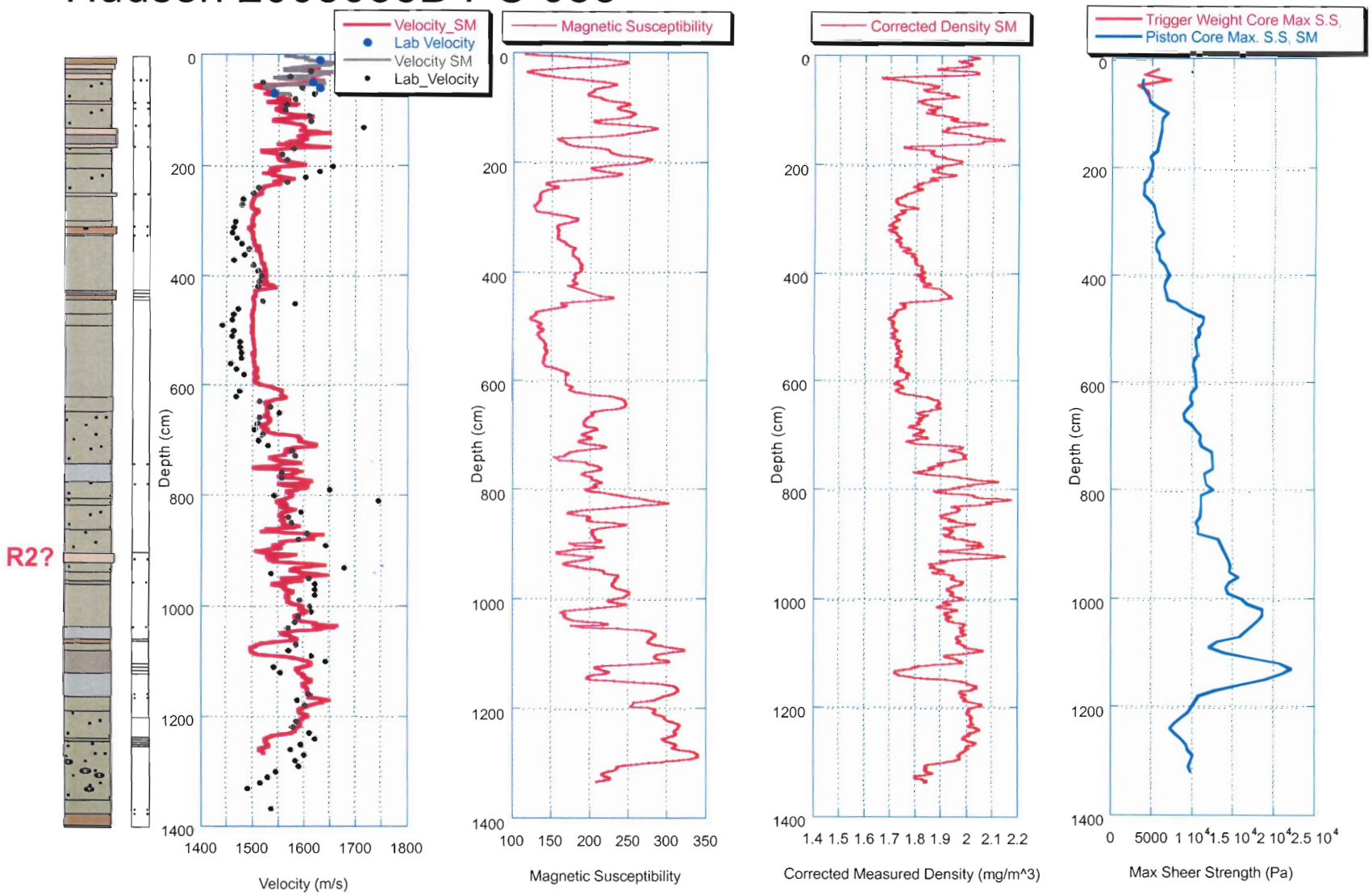

Color Plot 2005033B PC Core 51

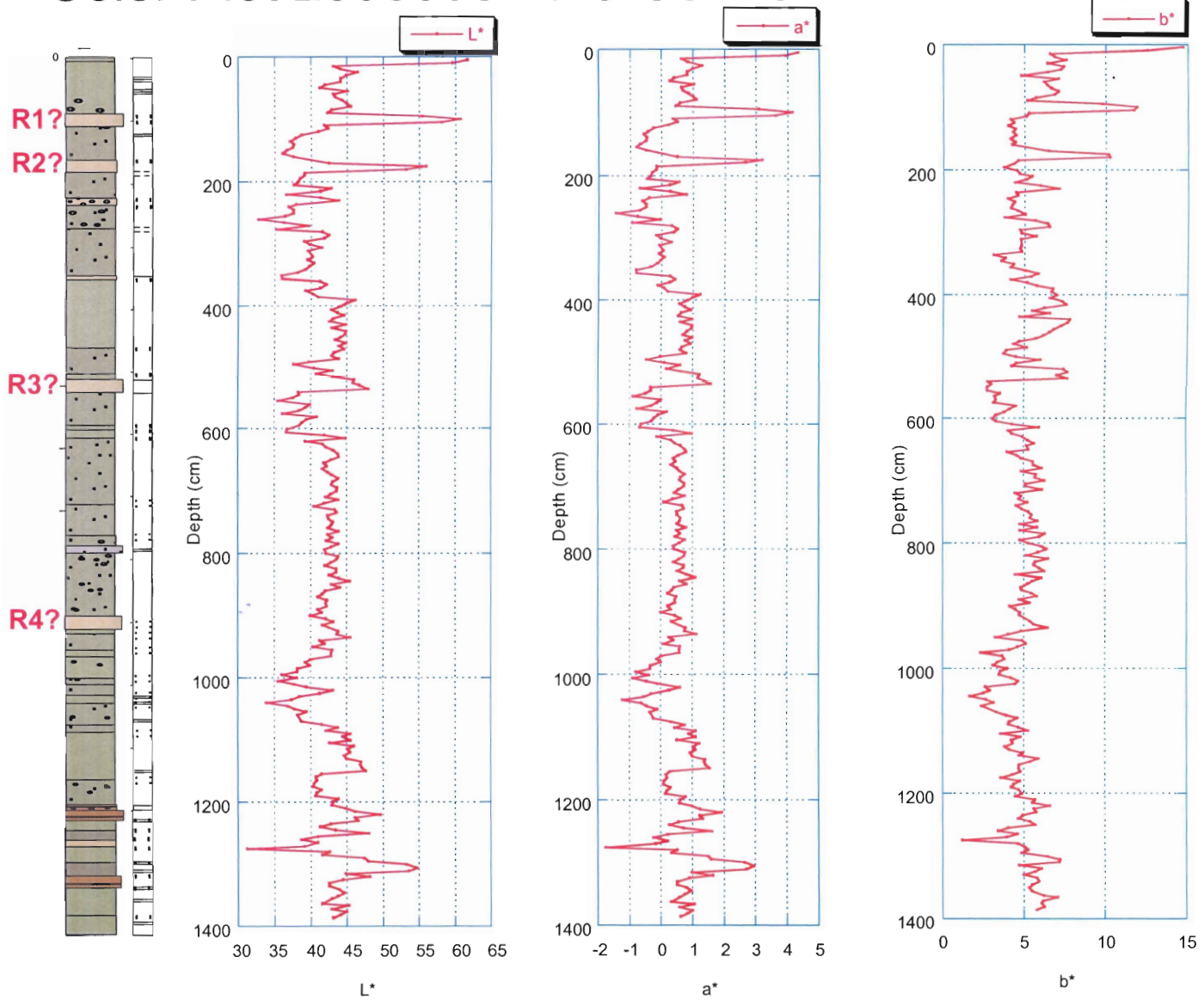

Color Plot 2005033B PC Core 52

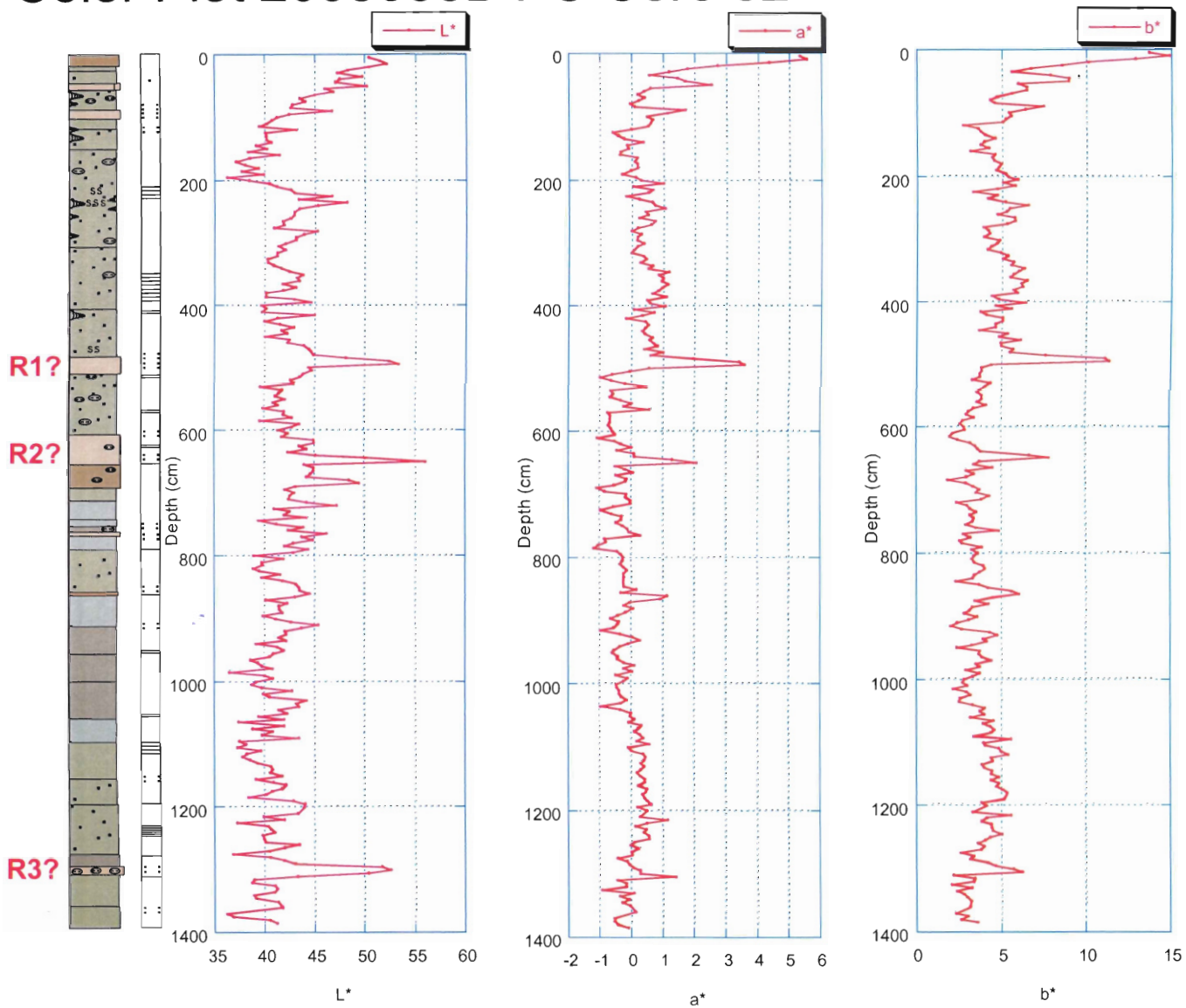

Color Plot 2005033B PC Core 53

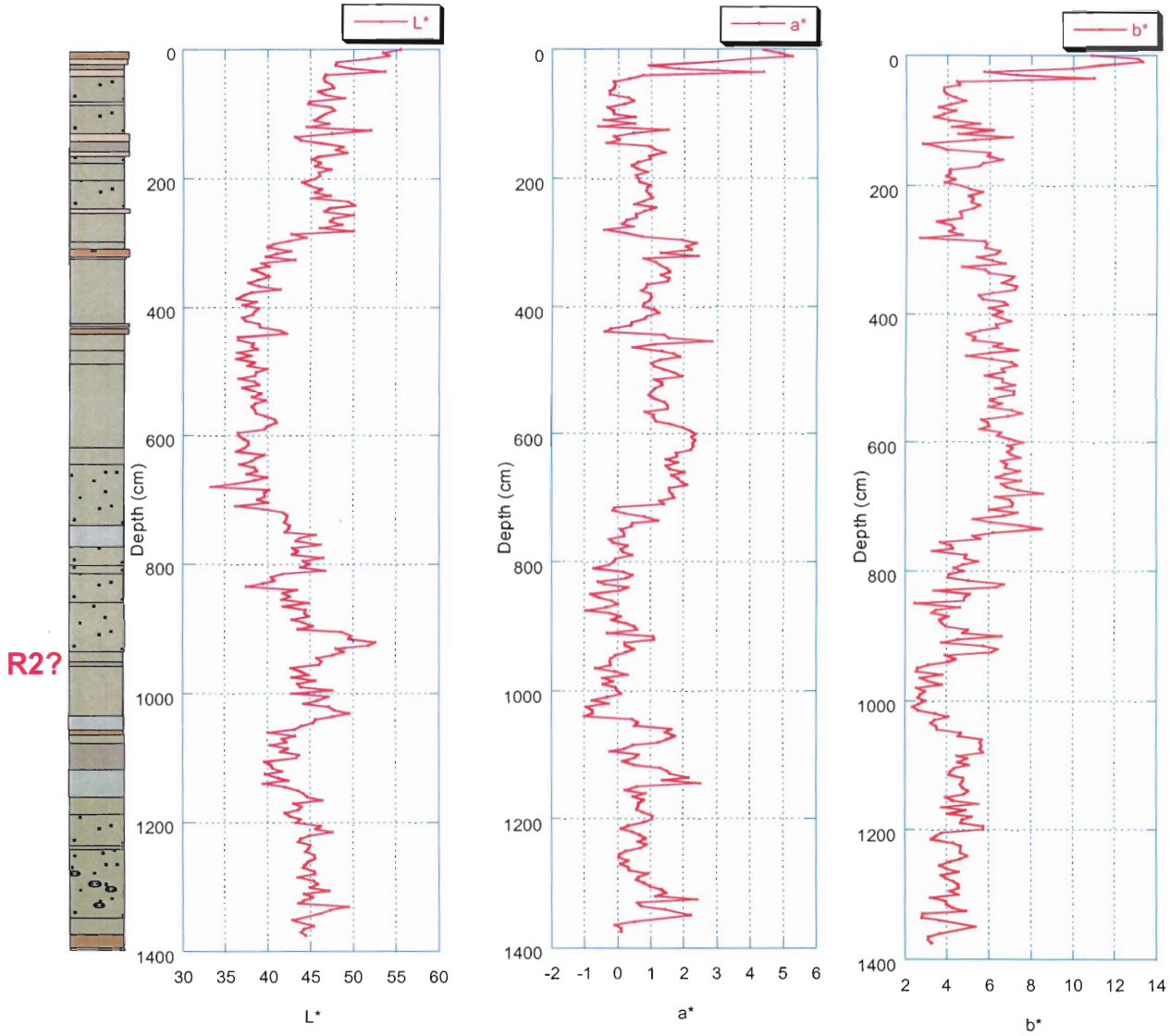

R2?

Hudson 2005033B TWC 51

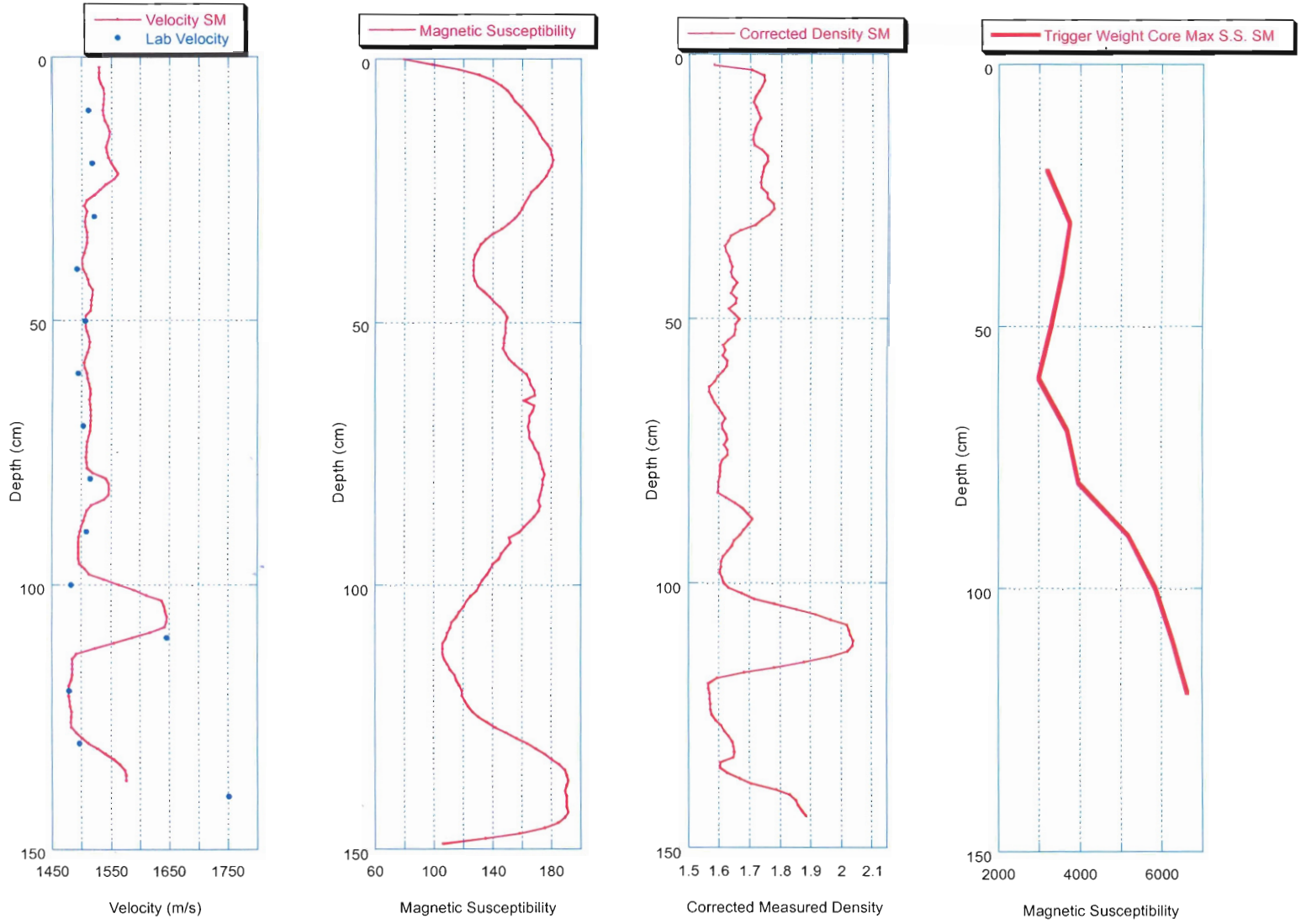

Hudson 2005033B TWC 52

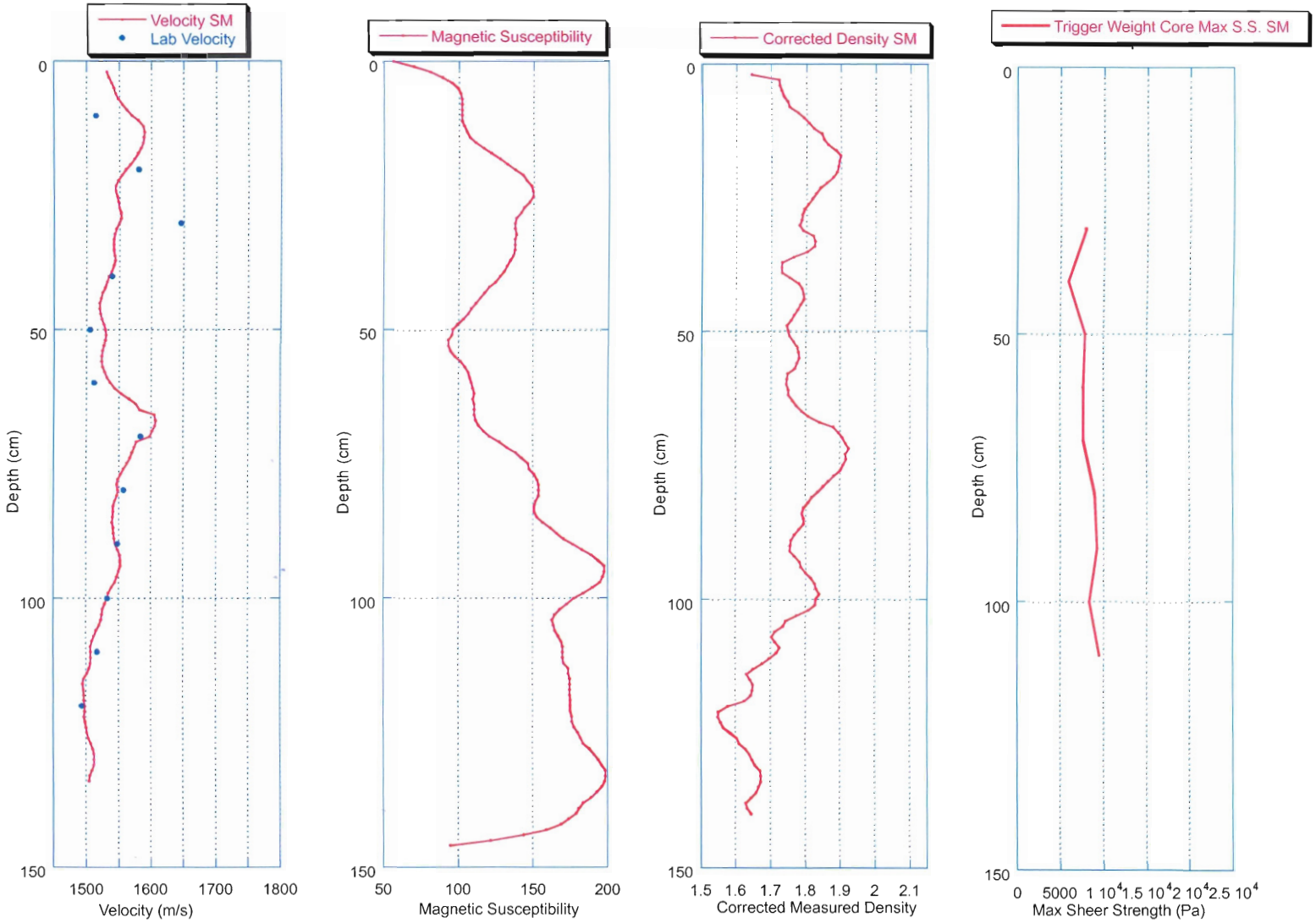

Hudson 2005033B TWC 53

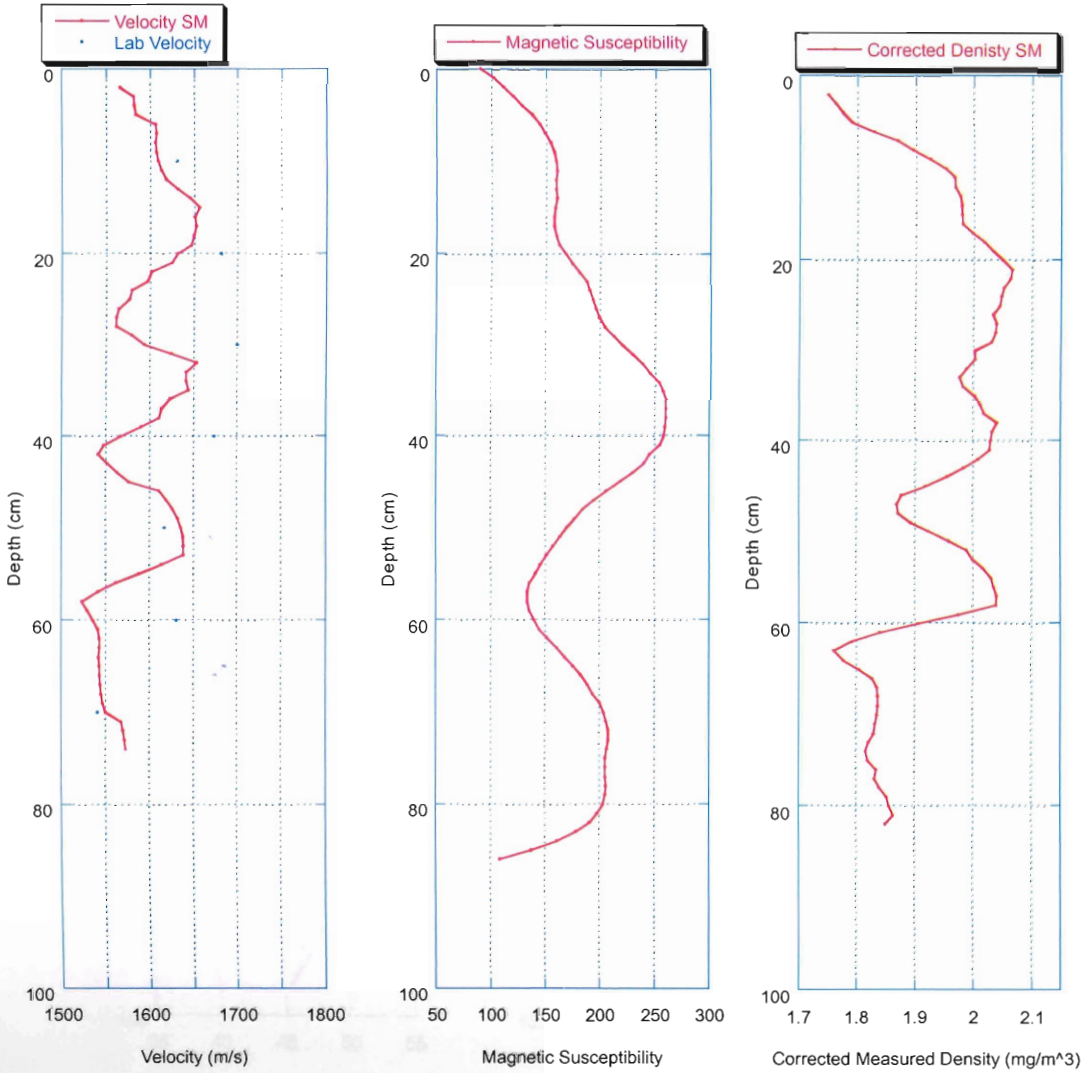

Color Plot 2005033B TWC Core 51

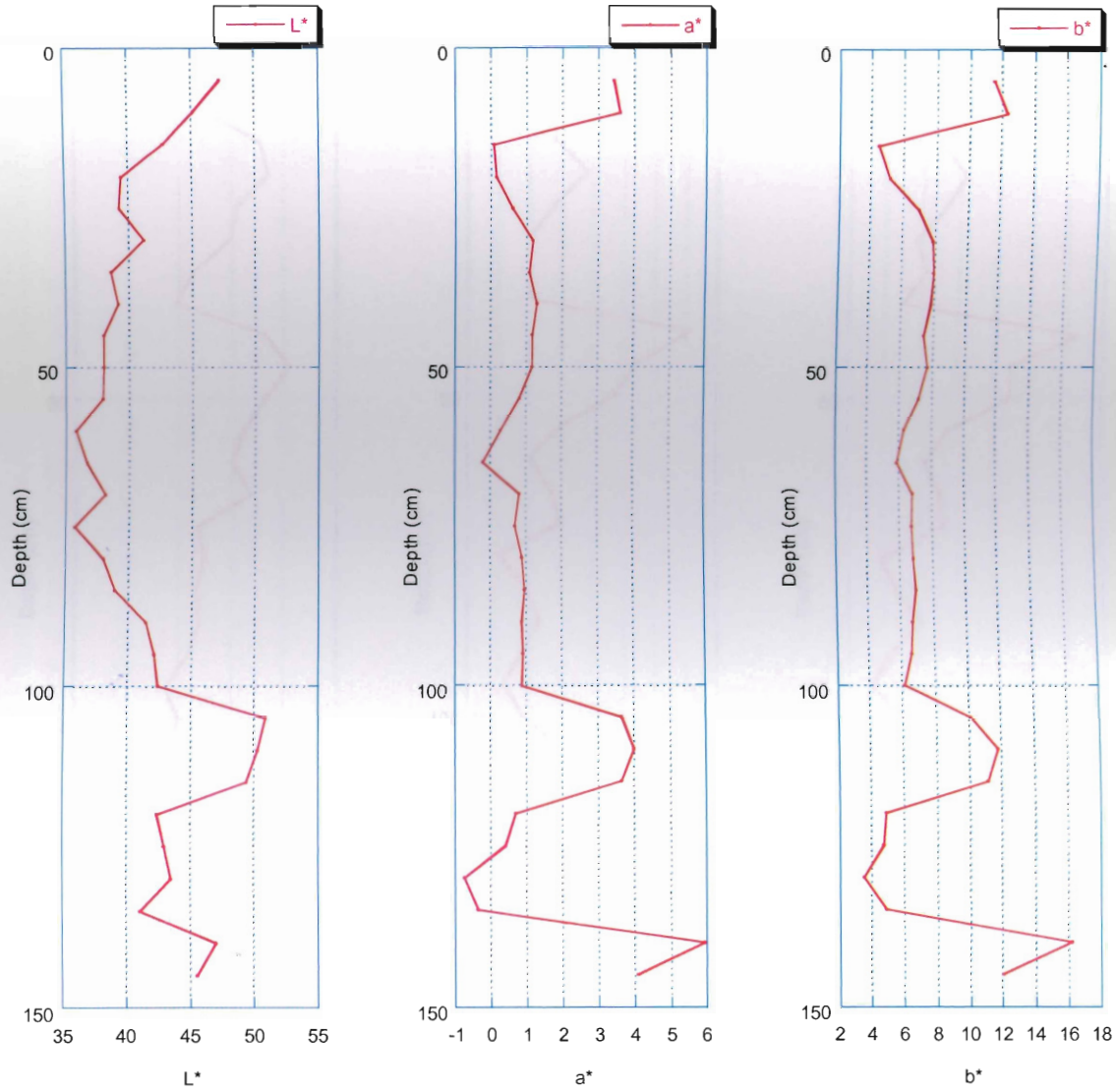

Color Plot 2005033B TWC Core 52

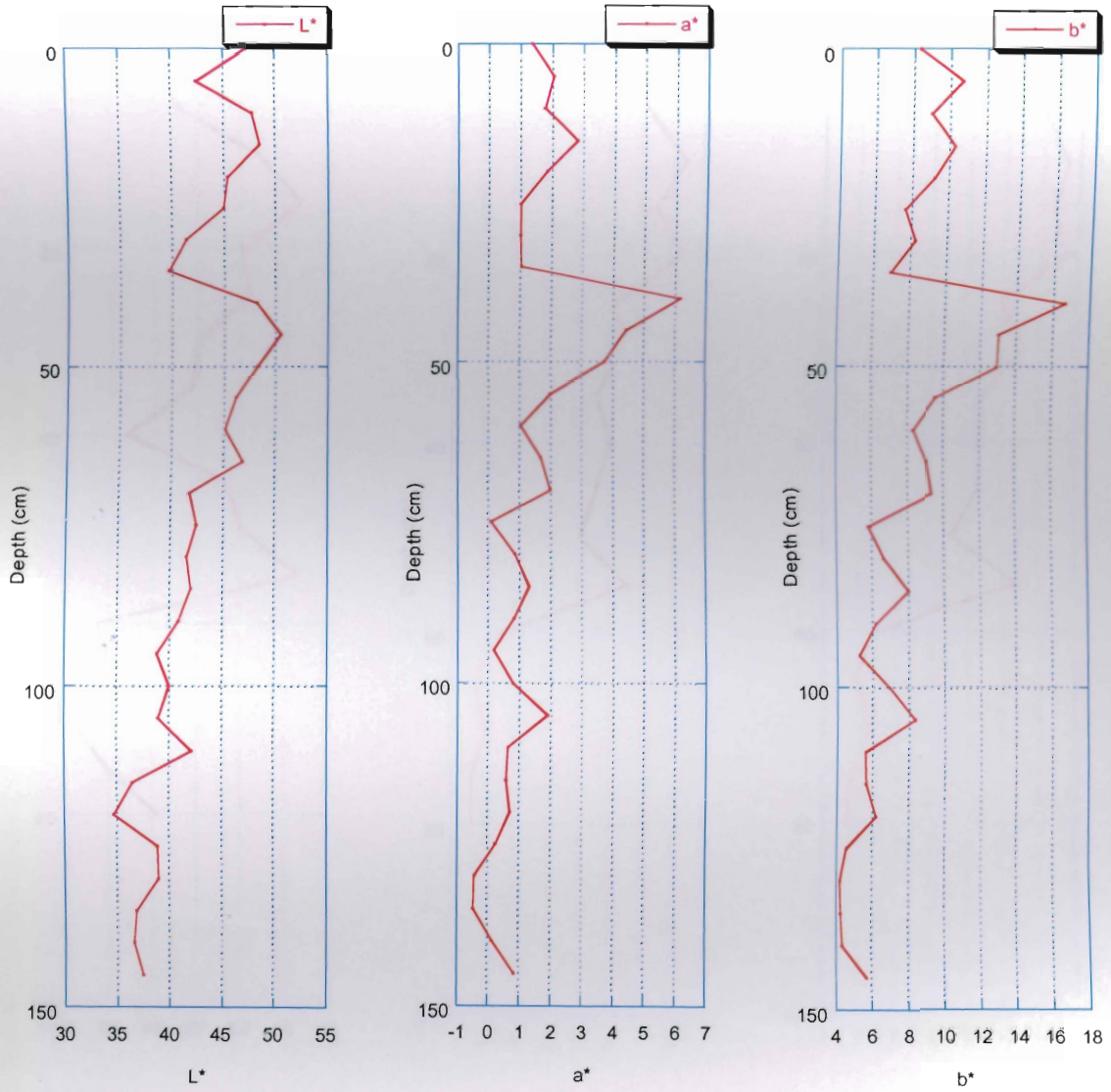

Color Plot 2005033B TWC Core 53